ISSN 007-2621

No. 4 — 1985

published quarterly

Technical Review

To Advance Techniques in Acoustical, Electrical and Mechanical Measurement

Validity of Intensity Measurements

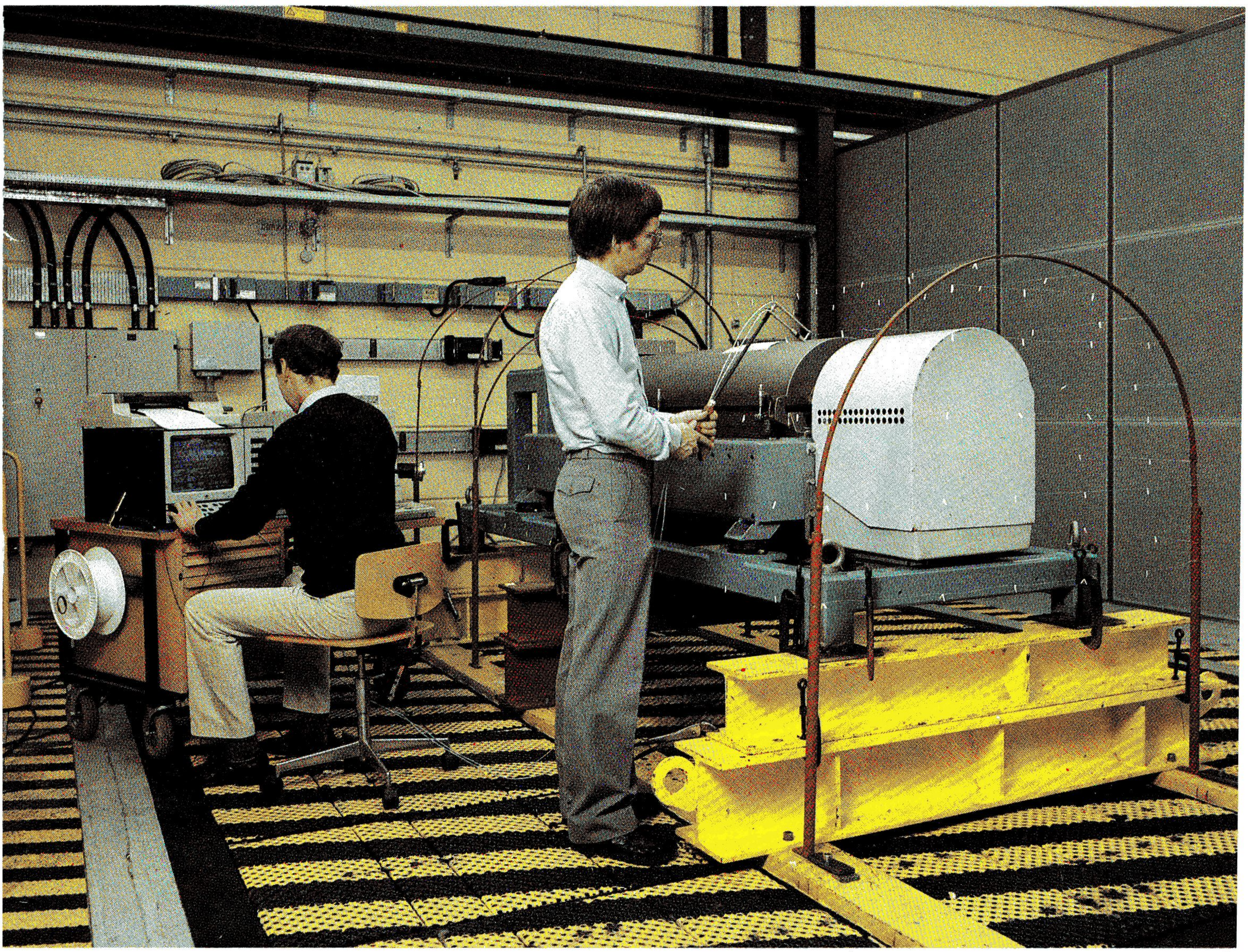

Influence of Tripods and Mic. Clips

Brüel & Kjær

PREVIOUSLY ISSUED NUMBERS OF BRÜEL & KJÆR TECHNICAL REVIEW

3-1985 The Modulation Transfer Function in Room Acoustics
RASTI: A tool for evaluating auditoria
2-1985 Heat Stress
A New Thermal Anemometer Probe for Indoor Air Velocity Measurements
1-1985 Local Thermal Discomfort
4-1984 Methods for the Calculation of Contrast
Proper Use of Weighting Functions for Impact Testing
Computer Data Acquisition from B & K Digital Frequency Analyzers 2131 / 2134 using their Memory as a Buffer
3-1984 The Hilbert Transform
Microphone System for Extremely Low Sound Levels
Averaging Times of Level Recorder 2317
2-1984 Dual Channel FFT Analysis (Part II)
1-1984 Dual Channel FFT Analysis (Part I)
4-1983 Sound Level Meters – The Atlantic Divide
Design principles for Integrating Sound Level Meters
3-1983 Fourier Analysis of Surface Roughness
2-1983 System Analysis and Time Delay Spectrometry (Part II)
1-1983 System Analysis and Time Delay Spectrometry (Part I)
4-1982 Sound Intensity (Part II Instrumentation and Applications)
Flutter Compensation of Tape Recorded Signals for Narrow Band Analysis
3-1982 Sound Intensity (Part I Theory).
2-1982 Thermal Comfort.
1-1982 Human Body Vibration Exposure and its Measurement.
4-1981 Low Frequency Calibration of Acoustical Measurement Systems. Calibration and Standards. Vibration and Shock Measurements.
3-1981 Cepstrum Analysis.
2-1981 Acoustic Emission Source Location in Theory and in Practice.
1-1981 The Fundamentals of Industrial Balancing Machines and their Applications.
4-1980 Selection and Use of Microphones for Engine and Aircraft Noise Measurements.
3-1980 Power Based Measurements of Sound Insulation.
Acoustical Measurement of Auditory Tube Opening.
2-1980 Zoom-FFT.
1-1980 Luminance Contrast Measurement.

(Continued on cover page 3)

TECHNICAL REVIEW

No. 4 — 1985

Contents

VALIDITY OF INTENSITY MEASUREMENTS IN PARTIALLY DIFFUSE SOUND FIELD

by

Svend Gade, M.Sc.

ABSTRACT

In this article a practical method is proposed and outlined for determining the Dynamic Capability of Intensity analyzing systems and the Reactivity Index of Intensity measurements. Furthermore, using this method, the amount of error due to phase mismatch, the amount of random error, and the useful frequency range for measuring intensity in different types of sound fields can be determined.

SOMMAIRE

Cet article propose et donne les grandes lignes d'une méthode pratique pour déterminer la capacité dynamique des systèmes d'analyse d'intensité acoustique et l'indice de réactivité des mesures d'intensité. De plus, en utilisant cette méthode, la valeur de l'erreur due au déphasage, la valeur de l'erreur aléatoire et la gamme de fréquence utile pour les mesures d'intensité dans les différents types de champ sonore peuvent être déterminées.

ZUSAMMENFASSUNG

In diesem Artikel wird eine praktische Methode zur Bestimmung der dynamischen Fähigkeiten und des Reaktivitätsindexes von Intensitätsmessungen vorgeschlagen und beschrieben. Außerdem läßt sich mit dieser Methode der Fehler durch Phasenfehlanpassung, der Zufälligkeitsfehler und der für verschiedene Schallfelder zulässige Frequenzbereich bestimmen.

Sound Intensity

Sound Intensity is a vector quantity, which describes the amount and the direction of net flow of acoustic energy at a given position.

It can be shown [1,13] that the intensity vector component in the direction r can be calculated from

$$I_r = -\frac{p^2_{rms}}{\rho c}\,\frac{1}{k}\,\frac{\partial \Phi}{\partial r} \qquad (1)$$

where $\partial\Phi/\partial r$ is the phase gradient of the sound field in the direction, r, p^2_{rms} is the mean square pressure, ρc is the impedance of the medium and k is the wave number.

Equation (1) shows that intensity calculations using the two-microphone method involves determination of the mean square sound pressure as well as the phase difference of the sound field between the two microphone positions. The critical point for sound intensity calculations is the phase measurement. The sound pressure is often taken as being the mean pressure value between the two microphone signals.

Bias Error, Approximation Error

For a plane (free field) sinusoidal wave, which propagates along the axis joining the microphones, the two-microphone method assumes that the free field phase between the two microphone positions is equal to $(k \cdot \Delta r)$, i.e. proportional to frequency and microphone spacing, while the measured free field phase is sin $(k \cdot \Delta r)$. Thus the measured intensity, $\hat{I}$, (see Fig.1) is related to the true intensity, I, [1] by:

$$\hat{I}/I = \sin(k \cdot \Delta r)/(k \cdot \Delta r) \qquad (2)$$

For sound intensity measurements in environments with diffuse background noise the approximation error appears to take the same form as for free field conditions [4,5]. This is because an intensity meter only responds to the propagating part (active part) of a sound field, and because the upper frequency limit, where the accuracy is within 1 dB, is found where the microphone spacing is approximately 6 times smaller than the apparent wavelength.

If there exists an angle, α, between the direction of propagation and the direction of probe orientation, r, the approximation error formula becomes

$$\hat{I}_\alpha = I_r \frac{\sin(k\Delta r \cdot \cos\alpha)}{k\Delta r} = I_\alpha \frac{\sin(k\Delta r \cdot \cos\alpha)}{k\Delta r \cdot \cos\alpha} \qquad (3)$$

As an example, if the angle, α, between the propagation of sound and the probe orientation is 60°, then the upper frequency limit for intensity

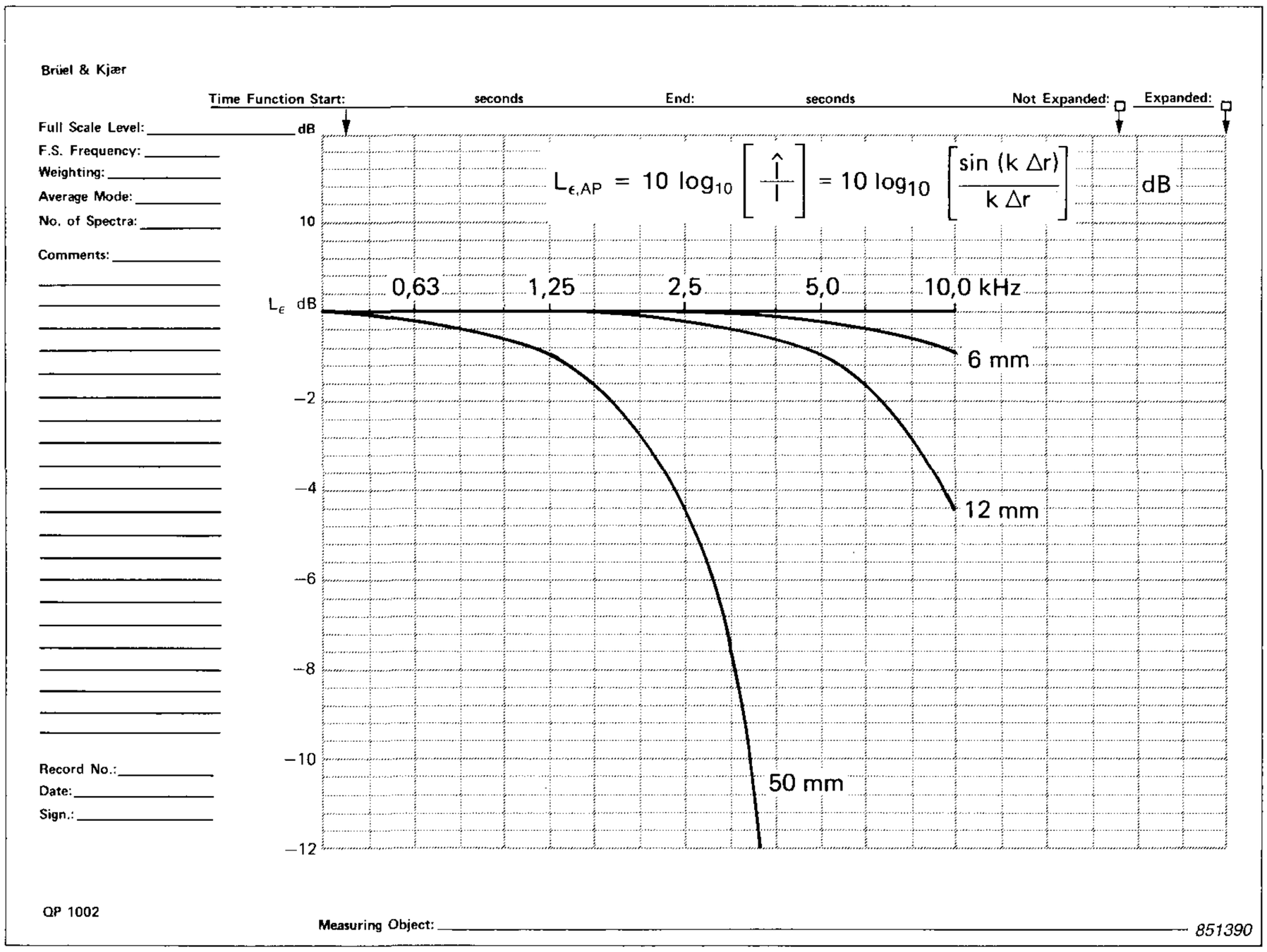

Fig. 1. Approximation error, $L_{\epsilon,AP}$, at high frequencies in an active sound field for various spacers

measurements is equal to twice the upper frequency limit as found when the angle, α, is 0°.

Since in a general sound field the direction of flow of acoustic energy might be different from microphone position to microphone position, any attempt to correct the measured intensity values by means of equation (2) would not be advisable. The formula only gives an idea of the upper frequency limit for a given microphone separation.

Intensity Index Nomogram

It can be shown [1,2,3,13] that in the frequency domain the intensity function can be calculated from the imaginary part of the cross-spectrum function, G_{AB}

$$\hat{I}(f) = -\frac{\text{Im } G_{AB}}{\omega \rho \Delta r} \tag{4}$$

where ω is the angular frequency and ρ is the density of the air.

The general formulation of the cross-spectrum is

$$G_{AB} = E[A^{\star} \cdot B]$$

$$= E[\,|A| \cdot |B| \cdot (\cos \Phi_{BA} + j \sin \Phi_{BA})] \qquad (5)$$

where E [ ] denotes expected value of the quantity inside the brackets. For simplicity we omit this symbol. The star * indicates a complex conjugate, that is a change of the sign of the imaginary part, which also corresponds to a change of the sign of the phase.

From (4) and (5) we have

$$\hat{I} \cdot \omega \rho \, \Delta r = |A| \cdot |B| \cdot \sin \Phi_{AB} \qquad (6)$$

For small angles $\sin \Phi_{AB} \approx \Phi_{AB}$. We also have that

$$|A| \cdot |B| \approx p^2_{rms}$$

Thus equation (6) can be rewritten as

$$\hat{I} \cdot kc \cdot \rho \cdot \Delta r = p^2_{rms} \, \Phi_{AB}$$

or

$$\frac{k \Delta r}{\Phi_{AB}} = \frac{p^2_{rms}/\rho c}{\hat{I}} \qquad (7)$$

which is the Intensity Index Nomogram relation.

Equation (7) could have been evaluated directly from equation (1) by a finite difference approximation of the phase gradient, $\partial \Phi / \partial r \approx - \Phi_{AB} / \Delta r$.

Equation (7) shows the general relation between the free field phase or relative frequency, ($k \Delta r$), wave number or frequency, k, microphone spacing, Δr, actual phase, Φ_{AB} (or just Φ), pressure, p^2_{rms}, and intensity, I, for an actual measurement.

When the propagating sound field of interest is contaminated by diffuse background noise the actual phase Φ is smaller than the corresponding free field phase $k \Delta r$.

The Reactivity Index, K is defined as

$$K = \frac{k \Delta r}{\Phi} \tag{8}$$

or in logarithmic form with $\rho c = 400$ and the usual reference quantities

$$L_K = -10 \log K = L_I - L_p \tag{9}$$

In most situations we have that $K \geqslant 1$ and thus $L_K \leqslant 0\,\text{dB}$.

The use of L_K was introduced by Roland [6]. The Intensity Index Nomogram relation is shown in graphical form in Fig.2. Note that these curves make no allowance for the finite approximation error at high frequencies.

The nomogram is very useful in evaluating errors due to phase mismatch. For a Reactivity Index of 0 dB (free field condition, $L_p = L_I$) it is seen that when using a 12 mm microphone spacing, the phase of the sound field between the two microphone positions is 10° at 800 Hz, 1° at 80 Hz and 0,1° at 8 Hz. Here we assume that the probe orientation is the same as the direction of propagation of sound.

With a Reactivity Index of −10 dB ($L_I = L_p - 10\,\text{dB}$), the measured phase is 1° at 800 Hz, and with a Reactivity Index of −20 dB the phase is only 0,1°.

It is also seen that for a Reactivity Index of 0 dB and a microphone spacing of 6 mm, the phase of the sound field between the two microphone positions is 5° at 800 Hz, 0,5° at 80 Hz and 0,05° at 8 Hz.

Evidently, a phase mismatch is most critical at low frequencies and for high reactivity indices of the measurements, and for small spacings between the two microphones. In fact the measured phase of the sound field should always be at least 5 times larger than the phase-mismatch of the system to ensure an accuracy better than ± 1 dB.

Note that in practice the Reactivity Index, L_K, is normally negative and indicates an important character of the sound field **as** it is measured. L_K is not a direct measure of how reactive the sound field is, or how much diffuse background noise is present. As an example of a highly reactive sound field, a standing wave can be used. It can be shown (Refs.[12,13] or see Appendix A) that in such a sound field the intensity is the geometrical mean value between the maximum mean square pressure

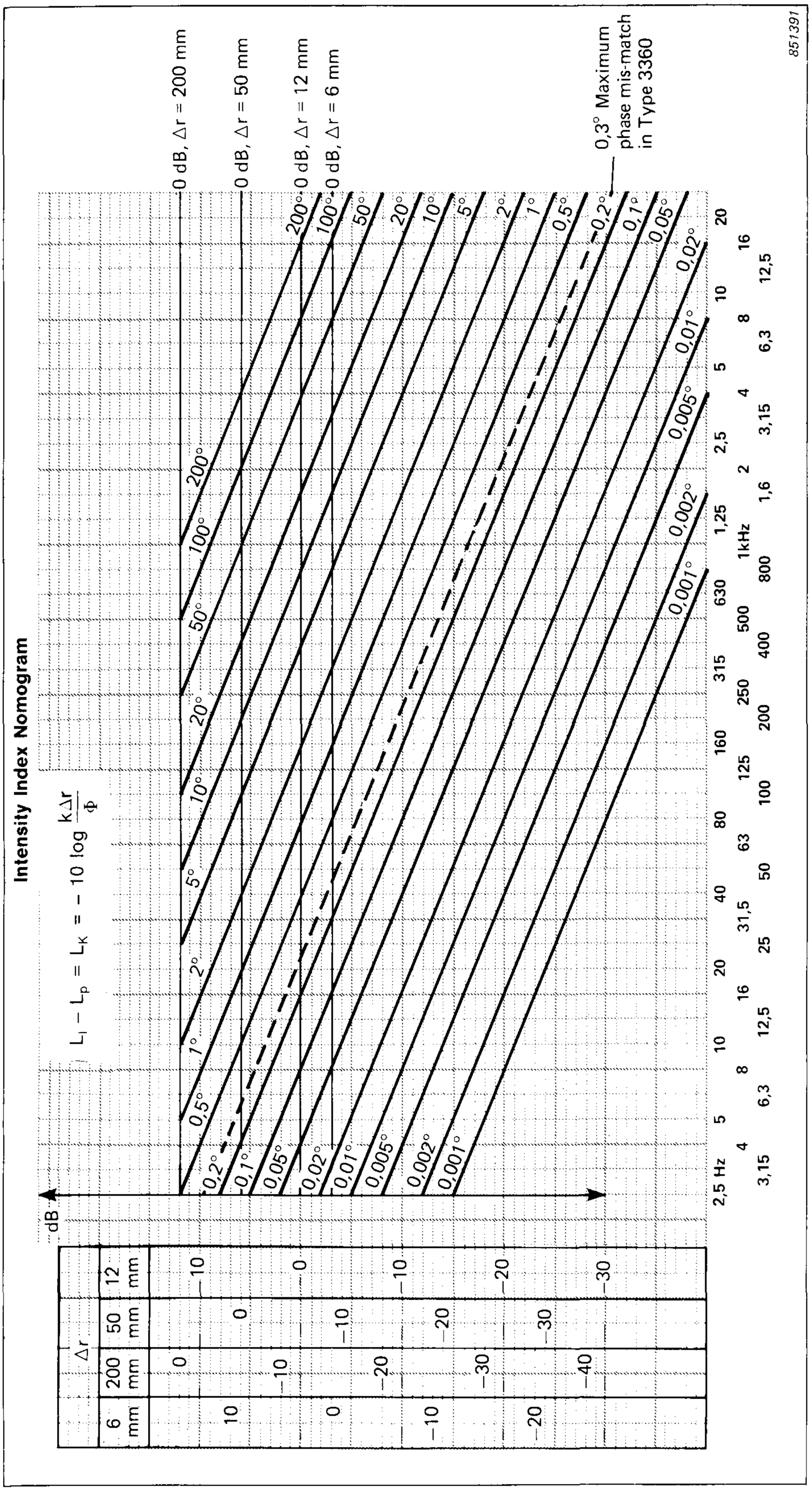

Fig. 2. The relation between frequency, Reactivity Index, phase and microphone spacing

and the minimum mean square pressure values normalized with respect to the impedance of the medium, ρc. In other words if the standing wave ratio is 20 dB, then L_K can take any value between –10 dB and + 10 dB depending on the observation position in the standing wave.

Also note that L_K cannot distinguish between different reasons for the measured phase. If L_p is 3 dB higher than the measured L_I the situation could be that we have

1) a plane propagating sound field, where the angle between the direction of propagation of sound and the direction of probe orientation is 60° or

2) a sound field consisting of two uncorrelated parts of equal strength, namely a plane propagating sound field and a diffuse sound field. In this case the direction of propagation of sound and the direction of probe orientation is assumed to be the same.

In the first case the upper frequency limit for the measuring system will be two times higher than in the latter case as discussed earlier.

In fact there exists an infinite amount of different combinations of active, reactive and diffuse sound fields where L_K is –3 dB.

All of the above discussion assumes that the intensity is determined without error.

Error due to Phase Mismatch

If the measured phase, $k\Delta r$, is small and if a phase mismatch, φ, exists between the two measuring channels, the relationship between the measured intensity, $\hat{I}$, and the true intensity, I, for free field conditions becomes

$$\hat{I}/I = \sin(k\Delta r \pm \varphi)/(k\Delta r)$$

$$\approx (k\Delta r \pm \varphi)/(k\Delta r) \qquad (10)$$

For the more general case, where free field conditions cannot be assumed, equation (10) becomes

$$\hat{I}/I \approx (\phi \pm \varphi)/\phi \qquad (11)$$

Using eqs.(8) and (9) the nomogram relation (7) can be written as

$$\Phi = 10^{(L_K/10)} \cdot (k \Delta r) \tag{12}$$

If a phase mismatch, φ, between the two channels exists and the phase difference of the sound field is ϕ, the measured phase becomes

$$\phi \pm \varphi = 10^{(L_K/10)} \cdot (k \Delta r) \tag{13}$$

If we feed the same broadband signal to the two measuring channels, we simulate a sound field with 0° phase difference between the two measurement positions [4,5,23,24]. In this case the difference between the measured intensity level (the Residual Intensity level, $L_{I,R}$, of the analyzing system) and the pressure level, $L_{p,R}$, is a measure of the phase mismatch, φ, between the two measuring channels and is, per definition, the Residual Intensity Index of the system, $L_{K,0}$.

$$L_{K,0} = L_{I,R} - L_{p,R} \tag{14}$$

From Equation (13), the phase mismatch between the two channels is given by

$$\varphi = 10^{(L_{K,0}/10)} \cdot (k \Delta r) \tag{15}$$

Solving equations (13) and (15) for ϕ gives

$$\phi = (10^{(L_K/10)} \mp 10^{(L_{K,0}/10)}) \cdot k \Delta r \tag{16}$$

Inserting equations (13) and (16) into (11) yields:

$$\hat{I}/I = 1/(1 \mp 10^{(L_{K,0} - L_K)/10}) \tag{17}$$

or in logarithmic form

$$L_{\epsilon,phase} = -10 \log [1 \mp 10^{(L_{K,0} - L_K)/10}] \tag{18}$$

Equations (17) and (18) indicate that the error due to phase mismatch only depends on the level difference between the Residual Intensity Index of the measuring system and the measured Reactivity Index of the sound field at the microphone positions.

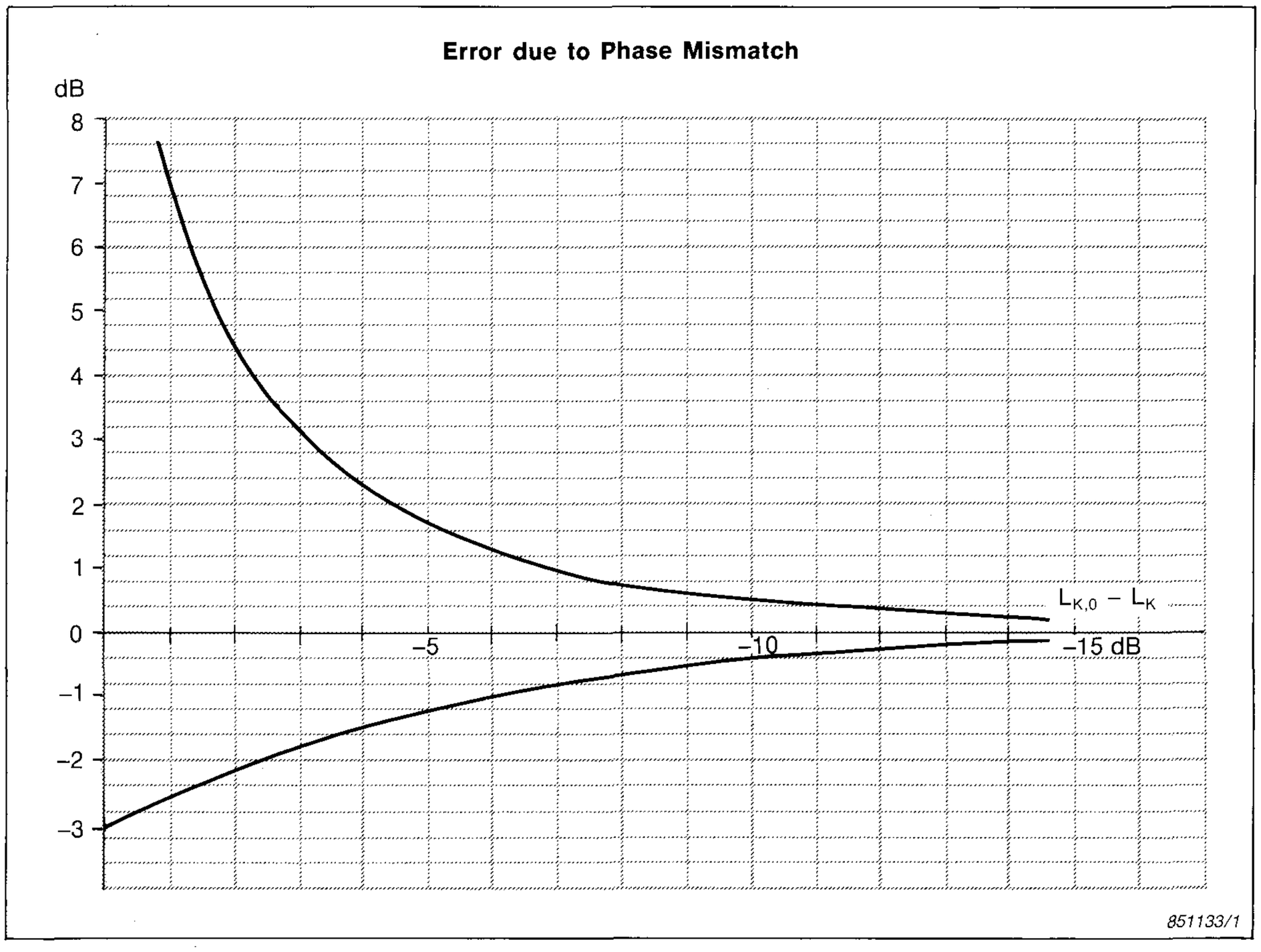

Fig. 3. Error due to phasemismatch for Intensity measurements

Equation (18) is derived in Appendix B without the use of the nomogram.

Fig.3 shows equation (18) in graphical form. The curves indicate that a measured Reactivity Index should be at least 7 dB higher than the Residual Intensity Index of the analysing system to ensure an error due to phase mismatch of less than $\pm$ 1 dB.

Thus we could define the Dynamic Capability of an Intensity Analyzing System by adding 7 dB to the Residual Intensity Index.

It should be noted that for most practical measurements all three quantities, Dynamic Capability, Reactivity Index and Residual Reactivity Index will be negative values.

The relationship between sound field and measurement system indicators for a given microphone spacing Δr using the two-microphone method is shown in Fig.4.

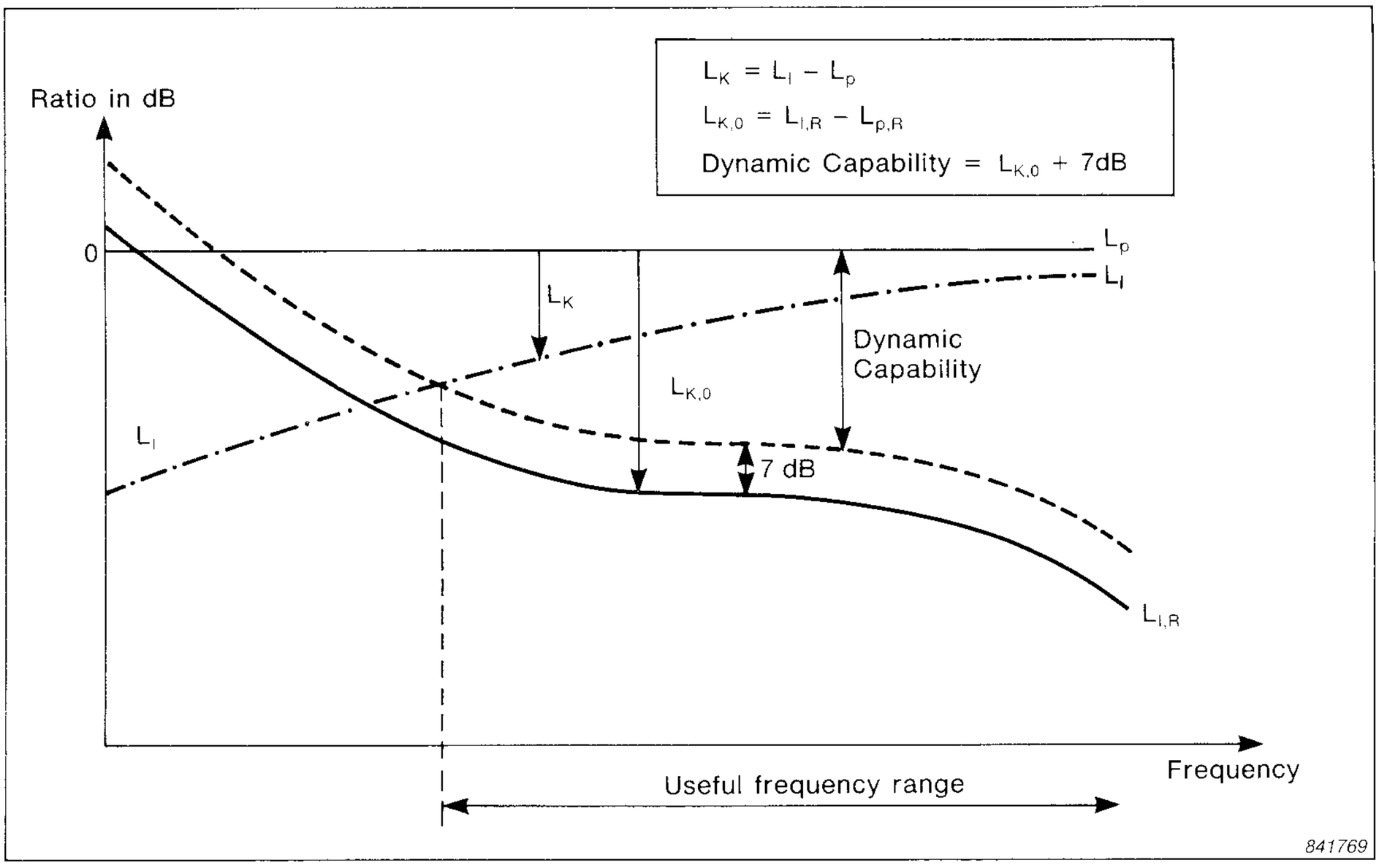

Fig. 4. Relationship between sound field and measurement system indicators where L_K is the Reactivity Index and $L_{K,0}$ is the Residual Intensity Index

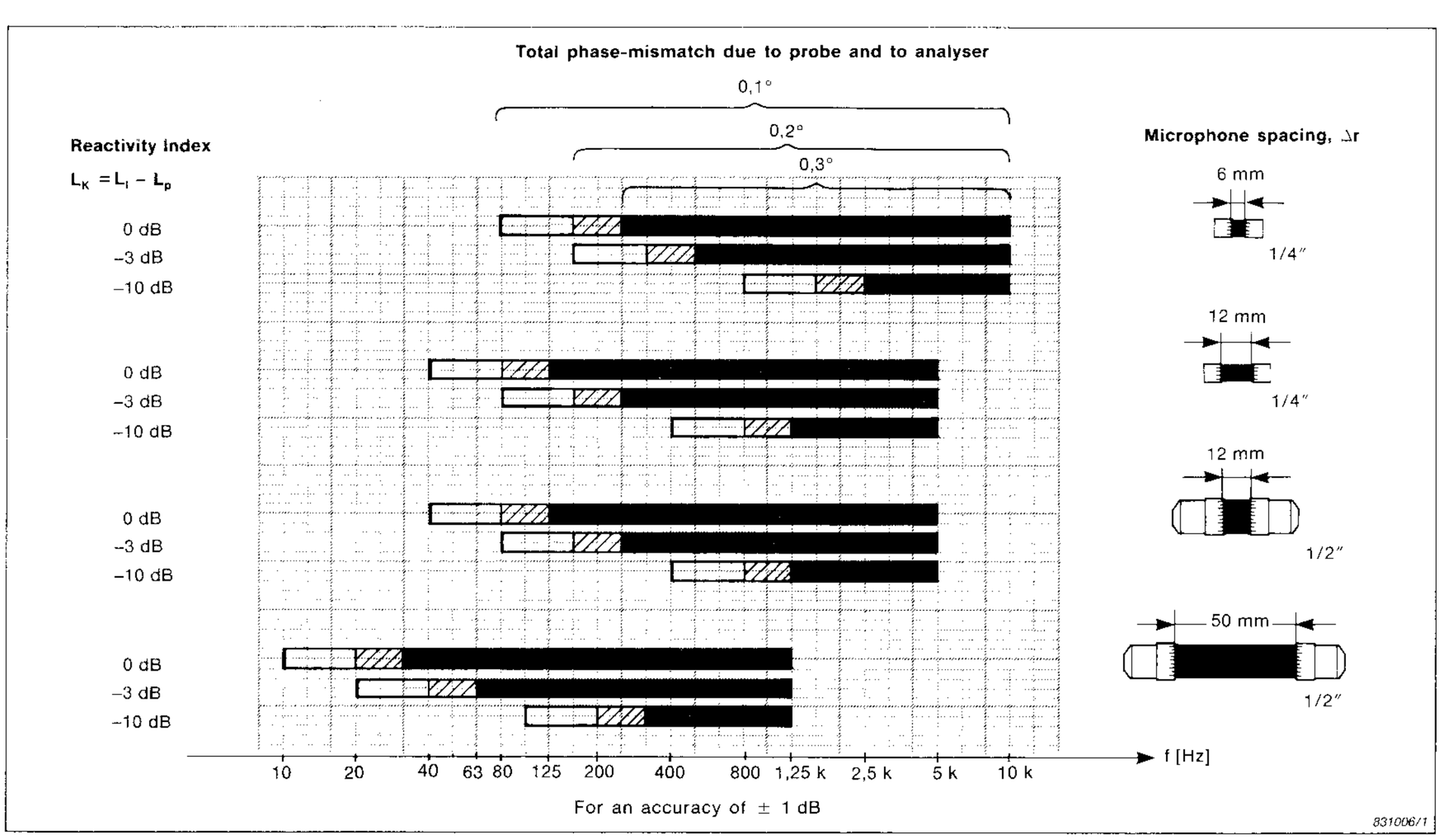

Fig. 5. The useful frequency range for various spacer configurations, phase-match and measured Reactivity Index for an accuracy of ± 1 dB

Note that increasing the microphone spacing will increase the Dynamic Capability but decrease both the upper and the lower frequency limit for the system. Thus the nomogram can be used for calculation of the useful frequency range as shown in Fig.5.

Random Error

For sound pressure measurements the normalized random error (68% confidence interval) is inversely proportional to the square root of the *BT* product (Bandwidth multiplied by Averaging Time) for $BT \geqslant 10$.

$$\epsilon_{random}\,[p^2_{rms}] \cong 1/\sqrt{BT} \tag{19}$$

For Sound Intensity measurements an equivalent formula exists. From [7] or from Appendix C we have

$$\epsilon_{random}\,[I] \cong (1/\sqrt{BT}) \cdot \sqrt{1 - \left((1-\gamma^2)/2\gamma^2\right)/\sin^2\Phi} \tag{20}$$

where γ^2 is the coherence function between the two signals at the positions of the microphones. A simple model [8,9] is used for calculation of γ^2 and Φ for Sound Intensity measurements, where the sound source of interest is regarded as a point source uncorrelated with the diffuse background noise.

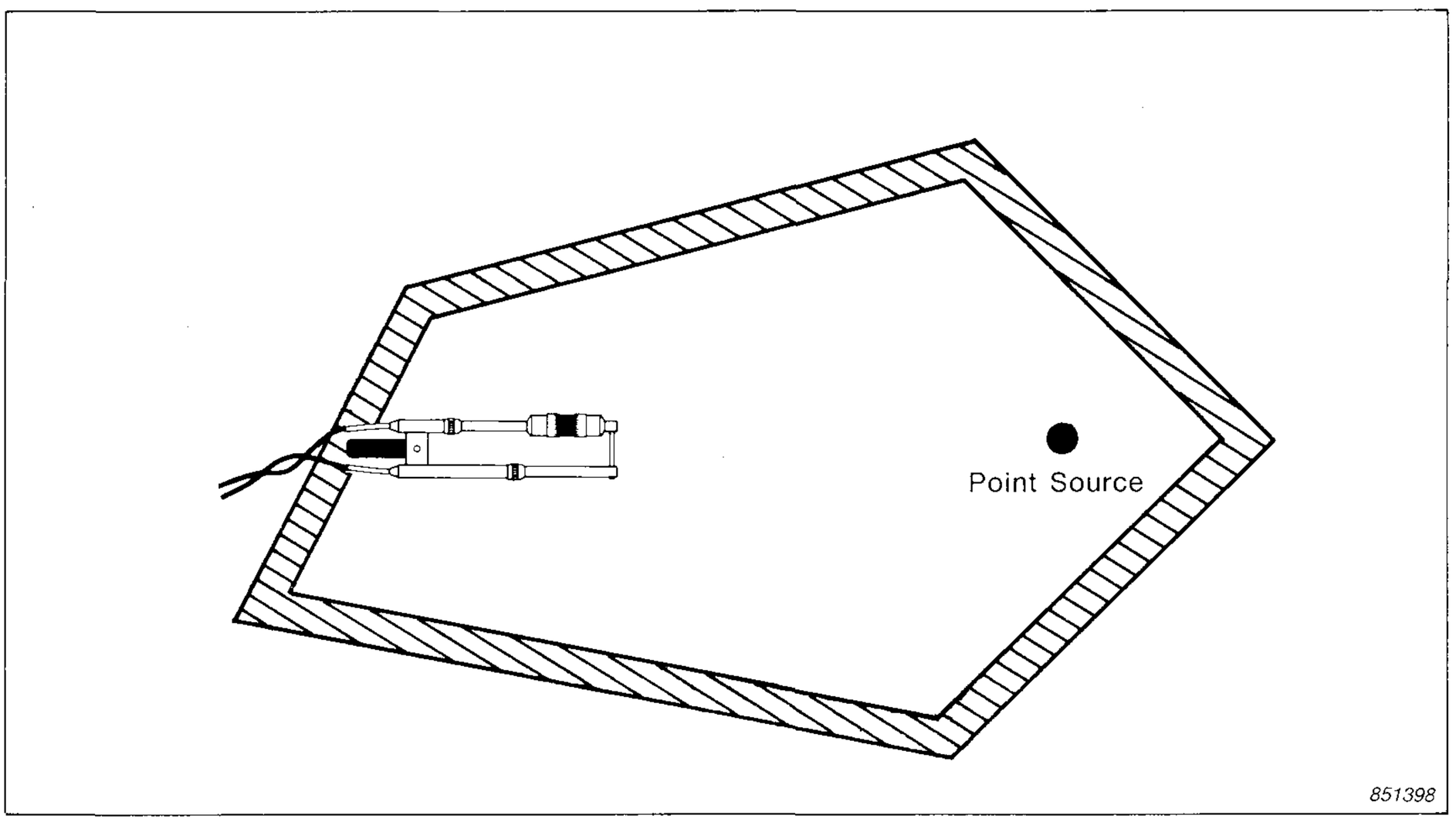

Fig. 6. Measurement of sound Intensity from a point source situated in environments with diffuse background noise

For simplicity the sound source of interest is situated in the direction where the microphone probe has maximum sensitivity, see Fig.6. However, this simplification does not impose any restriction on the orientation of the probe relative to the source, for measurements to be valid.

The measured Cross-spectrum due to the point source is

$$G_{AB} = G_{PP} [\cos (k \Delta r) + j \sin (k \Delta r)] \qquad (21)$$

where G_{PP} is the Autospectrum (the pressure spectrum).

The measured Cross-spectrum G_{AB} due to the diffuse background noise is:

$$G_{AB} = G_{DD} [\sin (k \Delta r)/(k \Delta r)] \qquad (22)$$

where G_{DD} is the Autospectrum (the pressure spectrum).

The resulting Cross-spectrum is the sum of the two Cross-spectra and the resulting Autospectrum is the sum of the two Autospectra. This is because the point source signal is uncorrelated with the diffuse background noise signal.

In this case the Reactivity Index is

$$K = \textit{Pressure/Intensity} = (G_{DD} + G_{PP})/G_{PP} \qquad (23)$$

Note that equation (23) also shows that the Reactivity Index, L_K, gives an indication of the Signal/Noise ratio for the measurements. As an example, when the propagating part of the sound field contributes 10% and the diffuse part of the sound field contributes 90% of the total sound pressure (or total energy density), L_K is –10 dB. In this case the Signal-/Noise ratio is –9,5 dB.

Using (21), (22) and (23) and $G_{AA} = G_{BB} = G_{DD} + G_{PP}$ we get

$$\gamma^2 = \frac{G_{AB}^2}{G_{AA} \cdot G_{BB}}$$

$$\approx |G_{AB}|^2/(G_{PP} + G_{DD})^2$$

$$= (1/K^2) [(\cos (k \Delta r) + (K-1) \cdot \sin (k \Delta r)/(k \Delta r))^2 + \sin^2 (k \Delta r)] \qquad (24)$$

and $\Phi \approx \tan^{-1} [\text{Im } G_{AB}/\text{Re } G_{AB}]$

$$= \tan^{-1} [\sin (k\Delta r)/(\cos (k\Delta r) + (K-1) \cdot \sin (k\Delta r)/(k\Delta r))] \quad (25)$$

Inserting equations (24) and (25) into (20) shows [8] that the required averaging time (BT-product) depends on the desired statistical accuracy, ϵ_r, and the Reactivity Index, K or L_K, but not on the relative frequency, $k\Delta r$ (the free field phase), in the frequency range of interest as shown in Fig.5, (see also Ref.[8]),

$$BT = f_1(\epsilon_r, \gamma^2, \Phi) = f_2(\epsilon_r, L_K) \quad (26)$$

The curves for 5%, 10%, 20% and 40% accuracy are shown in Fig.7.

These curves indicate that a change in Reactivity Index of –5 dB requires an increase in the averaging time by a factor of approximately 10 to yield the same statistical accuracy.

Fig.8 shows on linear axes $\epsilon_r[I] \cdot \sqrt{BT}$ as a function of K.

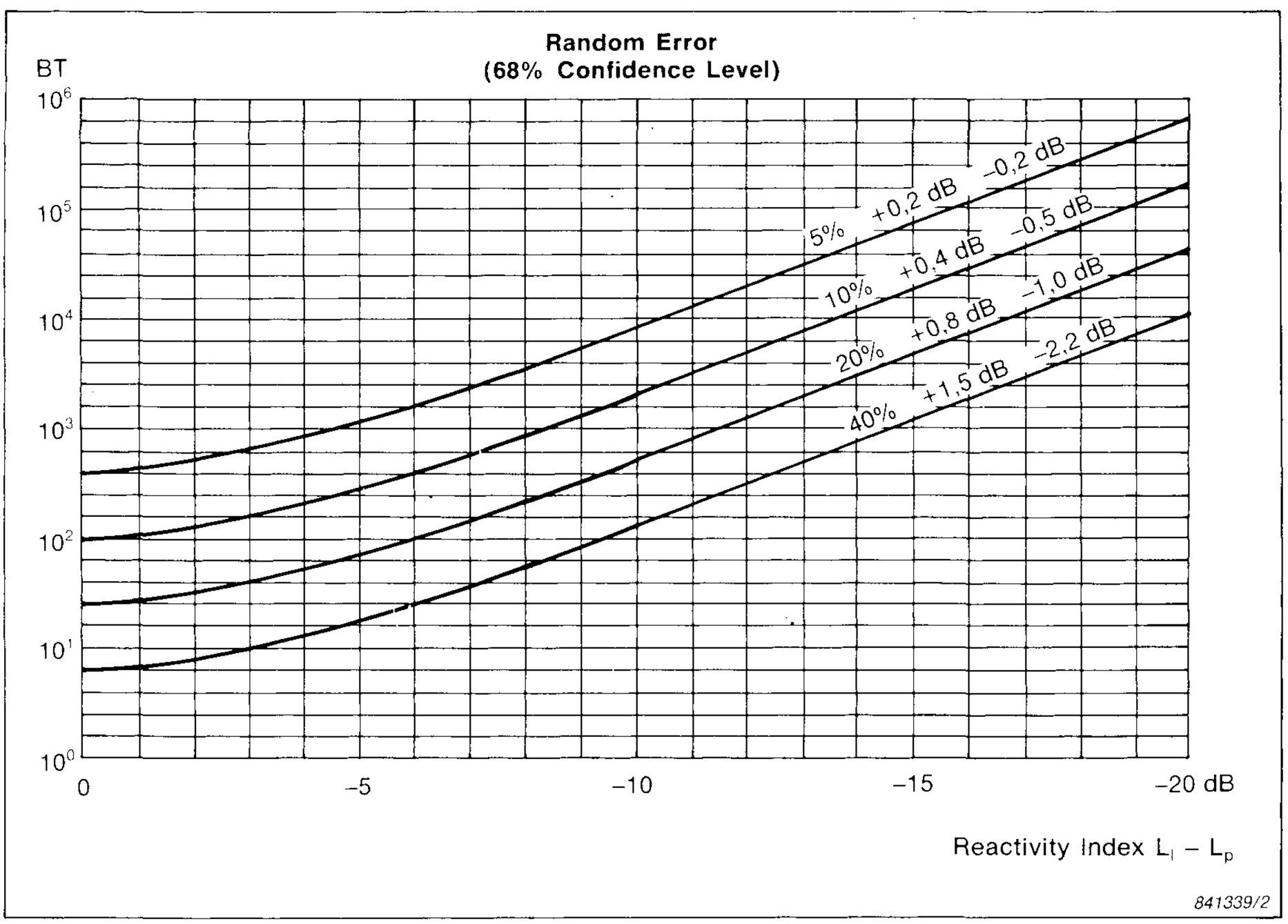

Fig. 7. Normalized random error (68% confidence interval) for Intensity measurements, diffuse background noise is assumed

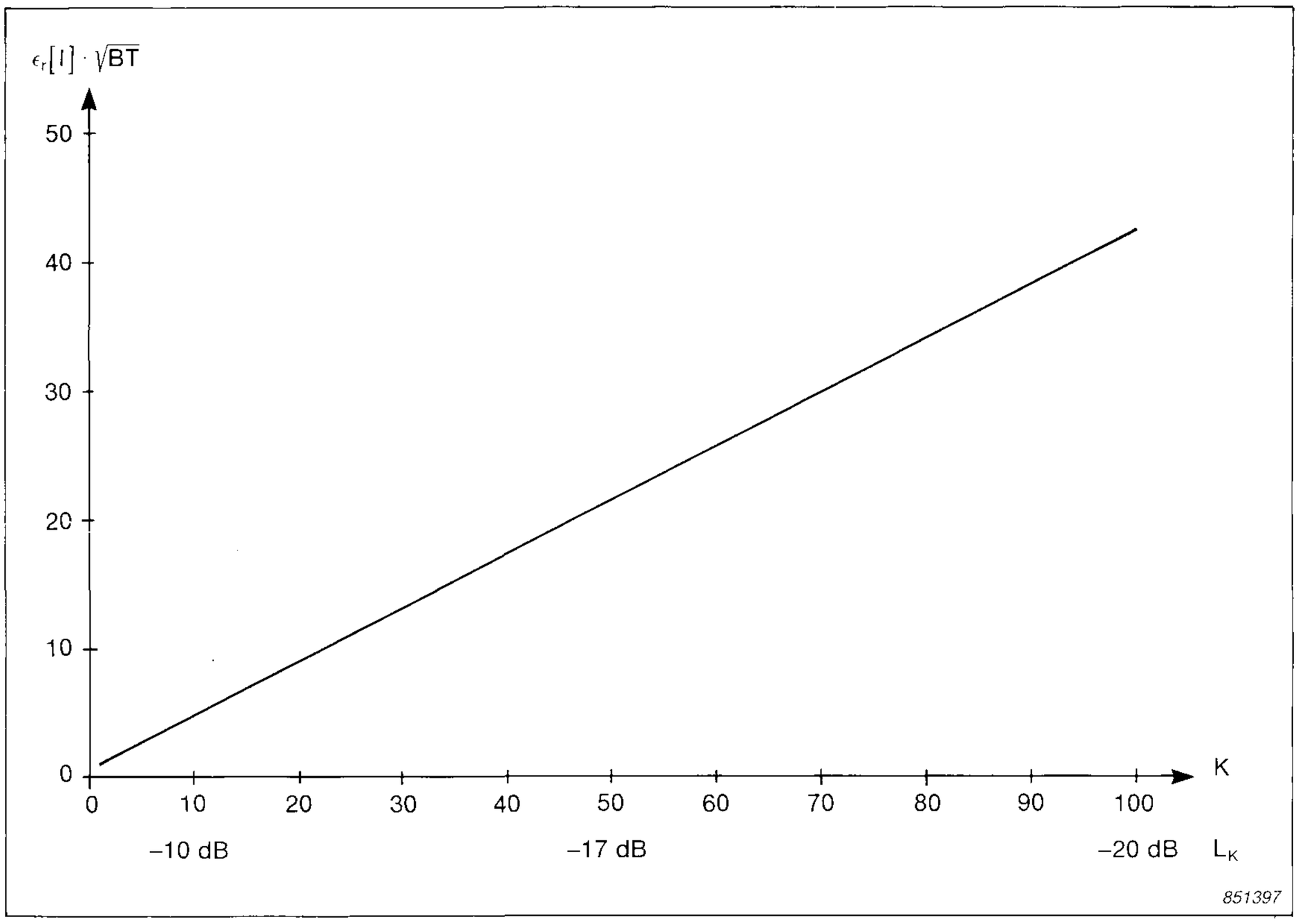

Fig. 8. Normalized random error (68% confidence interval) for Intensity measurements

The graph indicates a nearly perfect linear relationship between the two parameters.

For $K > 1$ we have

$$\epsilon_r[I] \cdot \sqrt{BT} \approx 0{,}42 \left(\frac{p^2_{rms}/\rho c}{I} + 1 \right)$$

$$\approx 0{,}42\,(K + 1) \qquad (27)$$

Sound Fields

At a given point in a sound field there will be an acoustic pressure, p, and a particle velocity, u. A natural way of classifying the sound field for intensity measurements is whether p and u are correlated or not.

The diffuse sound field is an example where p and u are uncorrelated. In this case there is no amplitude gradient or phase gradient of the sound field. All the energy is stored in the sound field.

Where p and u are correlated a further subdivision is possible. The situation where p and u are in phase can be defined as an active sound field. An example of a purely active sound field is a plane wave propagating in a free field. In this situation a phase gradient exists but no amplitude gradient. All acoustic energy propagates [1].

The situation where p and u are in quadrature, that is 90° out of phase, can be defined as a reactive sound field. An example of a purely reactive sound field is a standing wave. In this situation an amplitude gradient exists but no phase gradient. All energy fluctuates between the sources (real as well as imaginary sources) and the medium [1].

Note, that in general a sound field consists of an active, reactive and diffuse part. Also note that there might exist singular points in a sound field where the above definitions do not hold. One example is found where we have pressure maxima in an ideal, standing wave. In these points u is equal to zero – that is we have a purely pressure field. Another similar example is where we have velocity maxima in an ideal standing wave. In these points p is equal to zero – that is we have a purely velocity field. See A.1, A.2, A.3, see Refs.[25,26] for more information.

Note that in this paper we have used a mathematical model in which a point source emitting random noise is placed in a sound field contaminated with diffuse background noise for evaluation of finite difference approximation errors, errors due to phase mismatch and random errors for intensity measurements. Other models have also been used in Ref.[8].

As can be seen from this section, there is still a lot of work to be done before we have a model using a general sound field for evaluation of these errors, as well as errors for sound power determination using sound intensity measurements. Recent developments in this field are found in Refs. [15-22].

Conclusion

For intensity measurements in highly diffuse environments one must always measure the Residual Intensity Index, $L_{K,0}$ (or the Dynamic Capability) of the measuring system as well as the Reactivity Index, L_K of the sound field in the direction given by the microphone orientation at the point considered.

Error due to phase mismatch depends on the difference $L_{K,0} - L_K$ and random error depends on L_K as indicated in Fig.9.

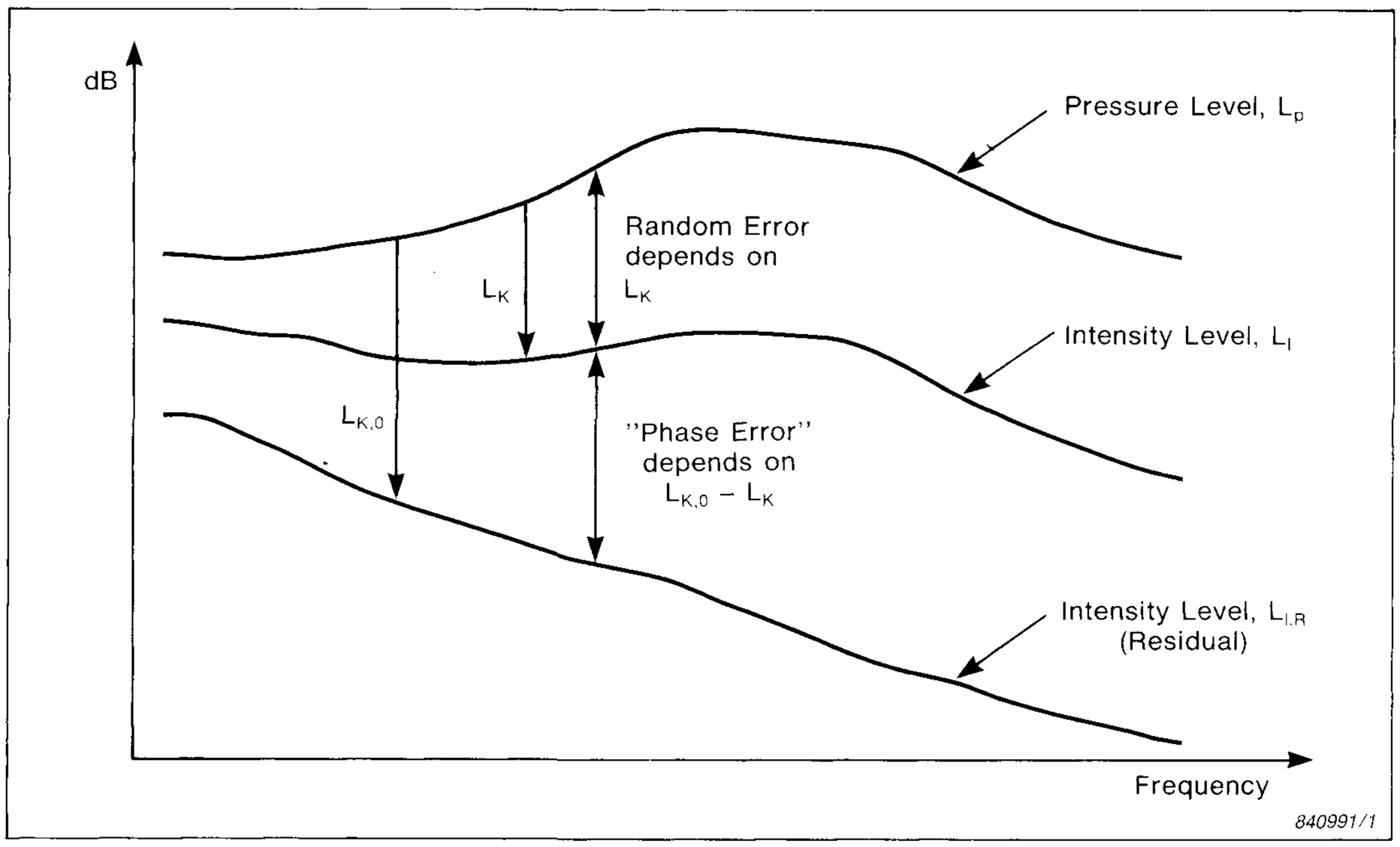

Fig. 9. Random error depends on the measured Reactivity Index of the sound field. Error due to phase mismatch depends on the difference between the measured Reactivity Index of the sound field and the Residual Intensity Index (Dynamic Capability) of the analyzing system

For the difference approximation error at high frequency it appears that the underestimation is similar to that under free field conditions.

A practical example where the outlined procedure for determining the validity of intensity measurements has been used is shown in Ref.[14]. Here measurements were performed inside a highly reactive and diffuse sound field, namely an empty aircraft in flight.

Acknowledgement

For useful discussions the author wishes to thank Dr. J. Pope and T.G. Nielsen M.Sc, Brüel & Kjær.

References

[1] GADE, S. "Sound Intensity (Theory, Instrumentation and Applications)", 1982, *B&K Technical Reviews,* Nos.3 & 4

[2] FAHY, F.J. "Measurements of Acoustic Intensity using the Cross Spectral Density of two Microphone Signals", 1977, *J. Acoust. Soc. Am.* 62 (4), pp.1057–1059

[3] CHUNG, J.Y. "Cross-Spectral Method of Measuring Acoustic Intensity", 1977, *GM Research Publication*, GMR–2617

[4] GADE, S., GINN, B., ROTH, O. & BROCK, M. "Sound Power Determination in Highly Reactive Environments", 1983, *Internoise Proceedings,* pp.1047–1050

[5] GADE, S., GINN, B., ROTH, O. & BROCK, M. "Sound Power Determination in Highly Reactive Environments", 1983, *B&K Application Note*. Extended version of [4]

[6] ROLAND, J. "What are the Limitations of Intensity Technique in a Hemi-diffuse Field", 1982, *Internoise Proceedings*, pp.715–718

[7] ELKO, G.W. "Frequency Domain Estimation of the Complex Intensity and Acoustic Energy Density", 1984, *Ph.D. Thesis, Pennsylvania State University,* pp.77–80, 328–332

[8] DYRLUND, O. "A Note on Statistical Errors in Acoustic Intensity Measurements", 1983, *Journal of Sound and Vibration*, 90, pp.585–589

[9] BENDAT, J.S., PIERSOL, A.G. "Engineering Applications of Correlation and Spectral Analysis", 1980, *New York, Wiley-Interscience*, pp.167–172

[10] JENKINS, G.M., WATTS, D.G. "Spectral Analysis", 1968, *San Francisco: Holden-Day*. Section 9.2.

[11] SEYBERT, A.F. "Statistical Errors in Acoustic Intensity Measurements", 1981, *Journal of Sound and Vibration*, 75, pp. 585–589

[12] SCHULTZ, J., SMITH Jr. P.W., MALME. C.I. "Measurement of Acoustic Intensity in Reactive Sound Field", 1975, *J.Acoust. Soc. Am.*, 67 (6), pp.1263–1268

[13] JACOBSEN, F. "Measurement of Sound Intensity", 1980, *The Acoustics Laboratory, Technical University of Denmark*, Report No.28

[14] GADE, S., NIELSEN, T.G. "Sound Intensity Measurements Inside Aircraft", 1985, *Eleventh European Rotorcraft Forum,* Paper no.9, *The City University, London, England*

[15] HÜBNER, G. "Development of Requirements for an Intensity Measurement Code Determinating Sound Power Level of Machines Under (Worst) In Situ Conditions", 1984, *Internoise Proceedings,* pp. 1093-1098

[16] RASMUSSEN, P. "Phase Errors in Sound Power Measurements", 1985, *Dept.13 Publication, Brüel & Kjær, Denmark*

[17] POPE, J. "Validity of Sound Power Determination using Sound Intensity Measurements", 1985, *Proceedings of 2nd International Congress on Acoustic Intensity,* pp.353–360

[18] NICOLAS, J., LEMIRE, G. "Precision of Active Sound Intensity Measurements in a Progressive and a Non Progressive Field", 1985, *J.Acoust. Soc. Am*, 78, pp.414–422

[19] NICOLAS, J., LEMIRE, G. "A Systematic Study of the Pressure-Intensity Index", 1985, *Internoise Proceedings*, pp.1179–1182

[20] NICOLAS, J., LEMIRE, G. "Comments on the Validity of the Index $L_I - L_p$", 1985, *Proceedings of the 2nd International Congress on Acoustic Intensity*, pp.337–342

[21] BOCKHOFF, M. "Sound Power Determination in the Presence of Background Noise", 1985, *Proceedings of the 2nd International Congress on Acoustic Intensity*, pp.275–282

[22] STIRNEMANN, A., BOLLETER, U., RATHE, E.J. "Possibilities and Limits of Sound Power Measurements with a Real-Time Intensity Analyzer", 1985, *Journal of Sound and Vibration*, 98 (3), pp.403–413

[23] FREDERIKSEN, E., "Phase Characteristics of Microphones for Intensity Probes", 1985, *Proceedings of the 2nd International Congress on Acoustic Intensity*, pp.23–30

[24] RASMUSSEN, G., BROCK, M. "Transducers for Intensity Measurements", 1983, *Proceedings of 11th International Congress on Acoustics*, vol.6, pp.177–180

[25] TICHY, J. "Use of the Complex Intensity for Sound Radiation and Sound Field Studies", 1985, *Proceedings of the 2nd International Congress on Acoustic Intensity*, pp.113–120

[26] PASCAL, J.C., LU, J. "Advantage of the vectorial nature of Acoustic Intensity to describe Sound Fields" 1984, *Internoise Proceedings*, pp.1111-1114

APPENDIX A

Reactivity Index in a Standing Wave

A standing wave consists of two plane waves travelling in opposite directions.

Thus using complex notation the instantaneous pressure as a function of time, t, and position, x, is

$$p = A\, e^{j(\omega t - kx)} + B\, e^{j(\omega t + kx)} \tag{A.1}$$

The instantaneous particle velocity can be calculated from eq. (A.2), Refs.[1,13]

$$u = -\frac{1}{\rho}\int \frac{\partial p}{\partial x}\, dt \tag{A.2}$$

which in this case gives $u = A\,\dfrac{k}{\omega\rho}\, e^{j(\omega t - kx)} - B\,\dfrac{k}{\omega\rho}\, e^{j(\omega t + kx)}$ (A.3)

The mean square pressure is

$$\begin{aligned}\overline{p^2} &= \frac{1}{2}\, p \cdot p^{\star} = \frac{1}{2}\,(A\, e^{-jkx} + B\, e^{+jkx})\,(A\, e^{+jkx} + B\, e^{-jkx}) \\ &= \frac{1}{2}\,(A^2 + B^2 + AB\, e^{-2jkx} + BA\, e^{2jkx}) \\ &= \frac{1}{2}\,(A^2 + B^2 + 2\,A \cdot B \cos 2kx)\end{aligned} \tag{A.4}$$

This means that $\overline{p^2}_{max} = \dfrac{1}{2}\,(A+B)^2$ *at antinode*, $kx = 0 + n\pi$ (A.5)

and $\overline{p^2}_{min} = \dfrac{1}{2}\,(A-B)^2$ *at node*, $kx = \pi/2 + n\pi$ (A.6)

The mean square particle velocity is

$$\overline{u^2} = \frac{1}{2}\, u \cdot u^{\star} = \frac{1}{2}\left(\frac{1}{\rho c}\right)^2 (A\, e^{-jkx} - B\, e^{jkx})\,(A\, e^{jkx} - B\, e^{-jkx})$$

$$= \frac{1}{2}\left(\frac{1}{\rho c}\right)^2 (A^2 + B^2 - AB\, e^{-j2kx} - AB\, e^{+j2kx})$$

$$= \frac{1}{2}\left(\frac{1}{\rho c}\right)^2 (A^2 + B^2 - 2AB \cos 2kx) \qquad \text{(A.7)}$$

This means that

$$\overline{u^2}_{min} = \left(\frac{1}{\rho c}\right)^2 \cdot \frac{1}{2}(A - B)^2 \quad \textit{at antinode, } kx = 0 + n\pi \qquad \text{(A.8)}$$

and $$\overline{u^2}_{max} = \left(\frac{1}{\rho c}\right)^2 \cdot \frac{1}{2}(A + B) \quad \textit{at node, } kx = \pi/2 + n\pi \qquad \text{(A.9)}$$

The pressure has maxima where velocity has minima and vica versa.

The time averaged intensity is

$$I = \mathrm{Re}\left[\frac{1}{2}\, p \cdot u^{\star}\right]$$

$$= \mathrm{Re}\left[\frac{1}{\rho c} \cdot \frac{1}{2}(A\, e^{-jkx} + B\, e^{jkx})(A\, e^{jkx} - B\, e^{-jkx})\right]$$

$$= \mathrm{Re}\left[\frac{1}{\rho c} \cdot \frac{1}{2}(A^2 - B^2 - AB\, e^{-j2kx} + AB\, e^{j2kx})\right]$$

$$= \mathrm{Re}\left[\frac{1}{\rho c} \cdot \frac{1}{2}(A^2 - B^2 + 2AB\, j\sin 2kx)\right]$$

$$= \frac{1}{\rho c} \cdot \frac{1}{2}(A^2 - B^2) = \frac{1}{\rho c} \cdot \frac{1}{2}(A + B)(A - B) \qquad \text{(A.10)}$$

Eq. (A.10) shows that the intensity is constant along the standing wave. Now we define the standing wave ratio, R, as

$$\frac{\overline{p^2}_{max}}{\overline{p^2}_{min}} = \frac{(A + B)^2}{(A - B)^2} = R^2 \qquad \text{(A.11)}$$

Using eqs. (A.5) and (A.10) we get $$\frac{\overline{p^2}_{max}/\rho c}{I} = \frac{A+B}{A-B} = R \qquad \text{(A.12)}$$

and using eqs. (A.6) and (A.10) we get $$\frac{I}{\overline{p^2}_{min}/\rho c} = \left(\frac{A+B}{A-B}\right) = R \qquad \text{(A.13)}$$

Combining eqs. (A.12) and (A.13) we get

$$I = \sqrt{(\overline{p^2}_{min}/\rho c) \cdot (\overline{p^2}_{max}/\rho c)} \qquad \text{(A.14)}$$

that the intensity is the geometrical mean value between the maximum and minimum mean square pressures normalized with respect to ρc.

Thus on a logarithmic (dB) scale the intensity level is the arithmetical mean value between the maximum and minimum sound pressure level. See also Refs. [12,13].

$$L_I = \frac{L_{p,max} + L_{p,min}}{2} \qquad \text{(A.15)}$$

Fig.A.1 shows pressure, intensity and velocity levels for the second mode in a tube where the standing wave ratio is 25 dB.

Fig.A.2 shows the phase difference between pressure and velocity for the same case. There is a maximum phase difference between the 2 quantities when their levels in dB are the same. For a standing wave ratio of 25 dB the phase difference is 83°. At these points the sound field is highly reactive.

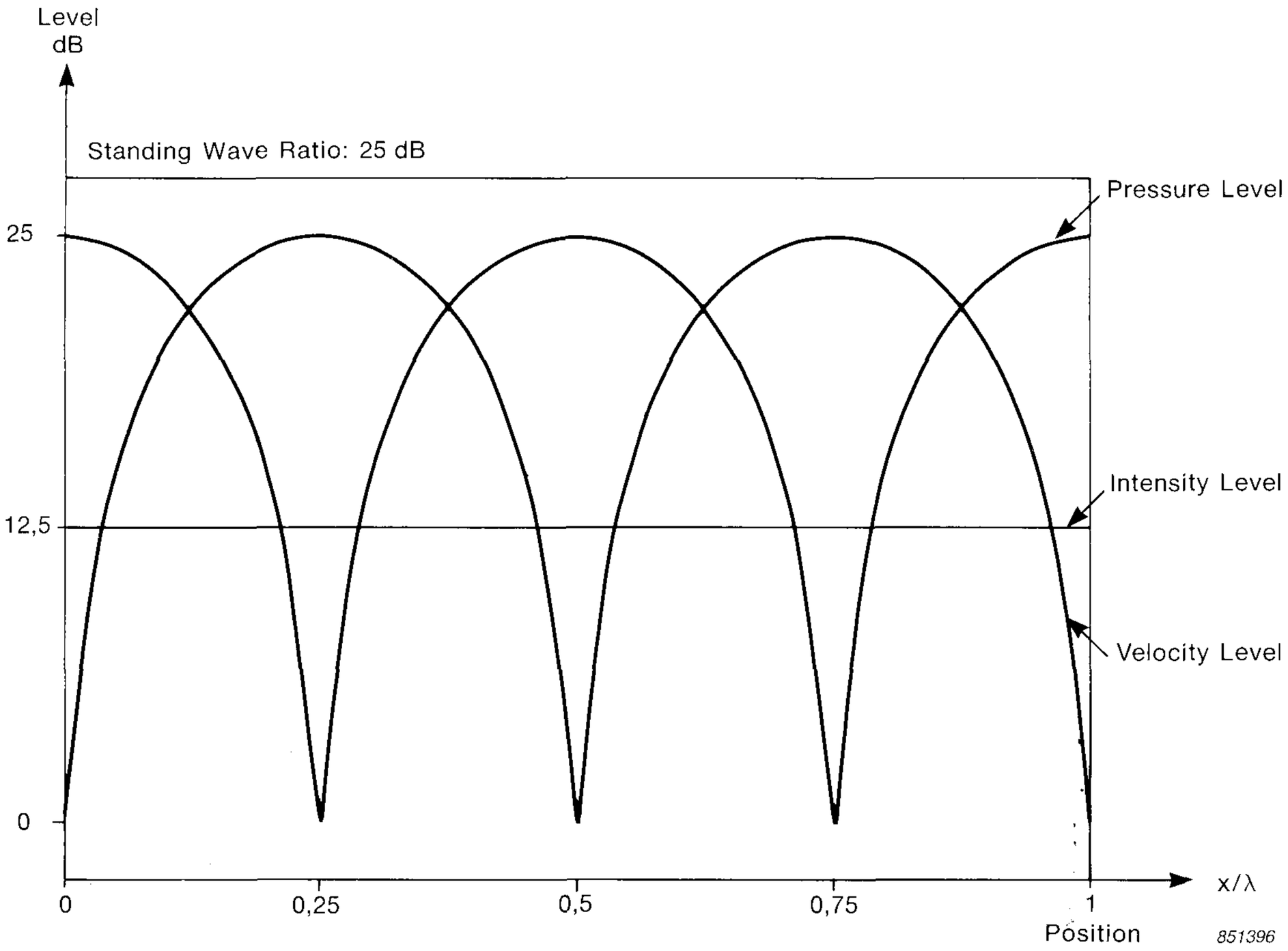

Fig. A.1. The level of pressure, Intensity and velocity for a standing wave, where the standing wave ratio is 25 dB. One wavelength is shown

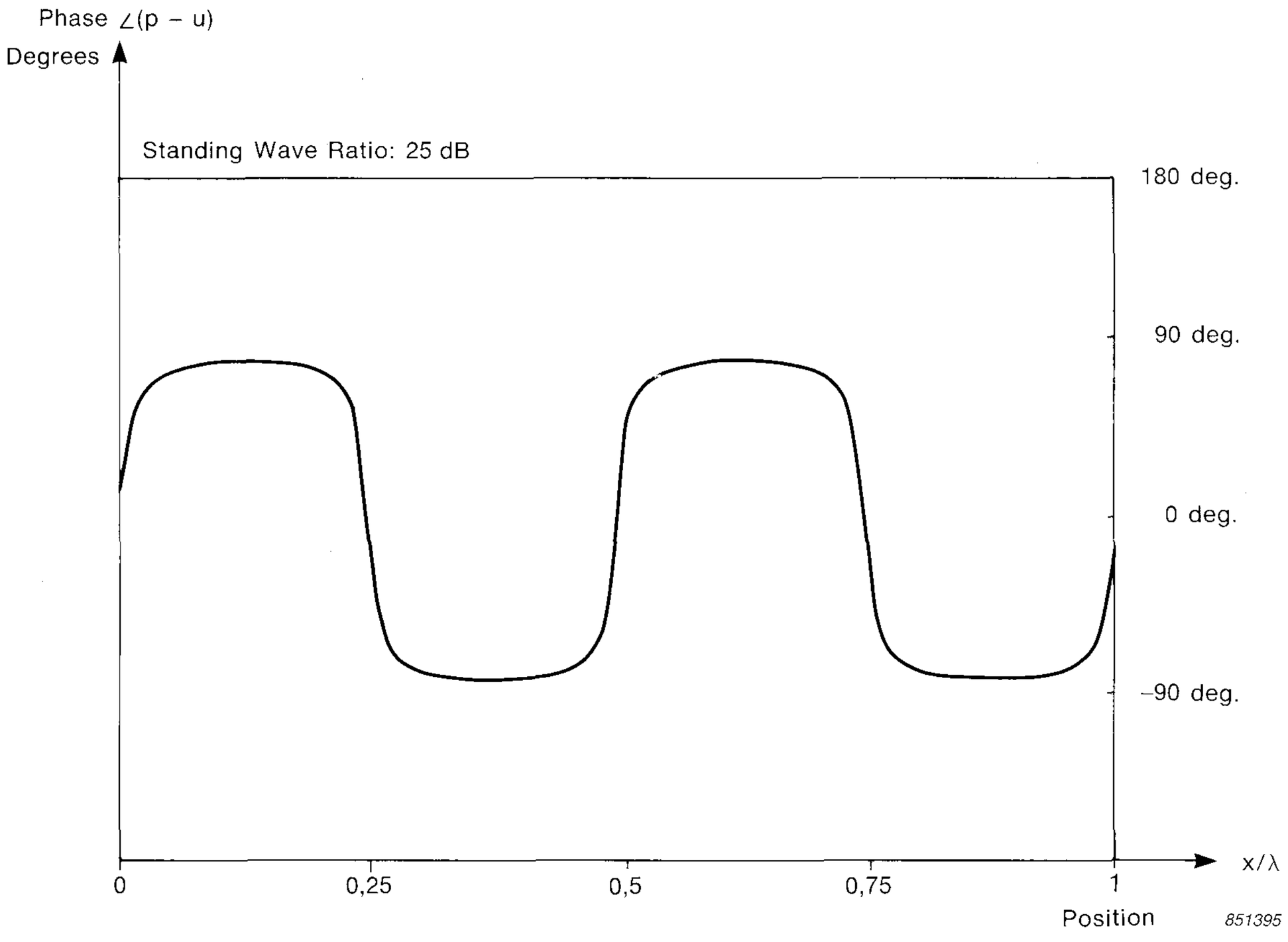

Fig. A.2. The phase difference between pressure and velocity for a standing wave, where the standing wave ratio is 25 dB. One wavelength is shown

Fig.A.3 shows pressure, intensity and velocity levels for the second mode in a tube where the standing wave ratio is 100 dB.

Where the pressure and the velocity have their maximum or minimum values the phase difference is 0°. At these points the sound field is purely active.

Figs.A.1 and A.3. also reveal that there are more positions in a standing wave where the pressure level is higher than the intensity level (L_K is negative) than where the intensity level is higher than the pressure level (L_K is positive).

Fig.A.4 shows the relative amount of positions in a standing wave as a function of standing wave ratio, where we have L_K positive.

In this Appendix reference values of $p_o = 20\,\mu Pa$, $u_o = 50$ nm/s, and $I_o = 1\,pW/m^2$ have been used.

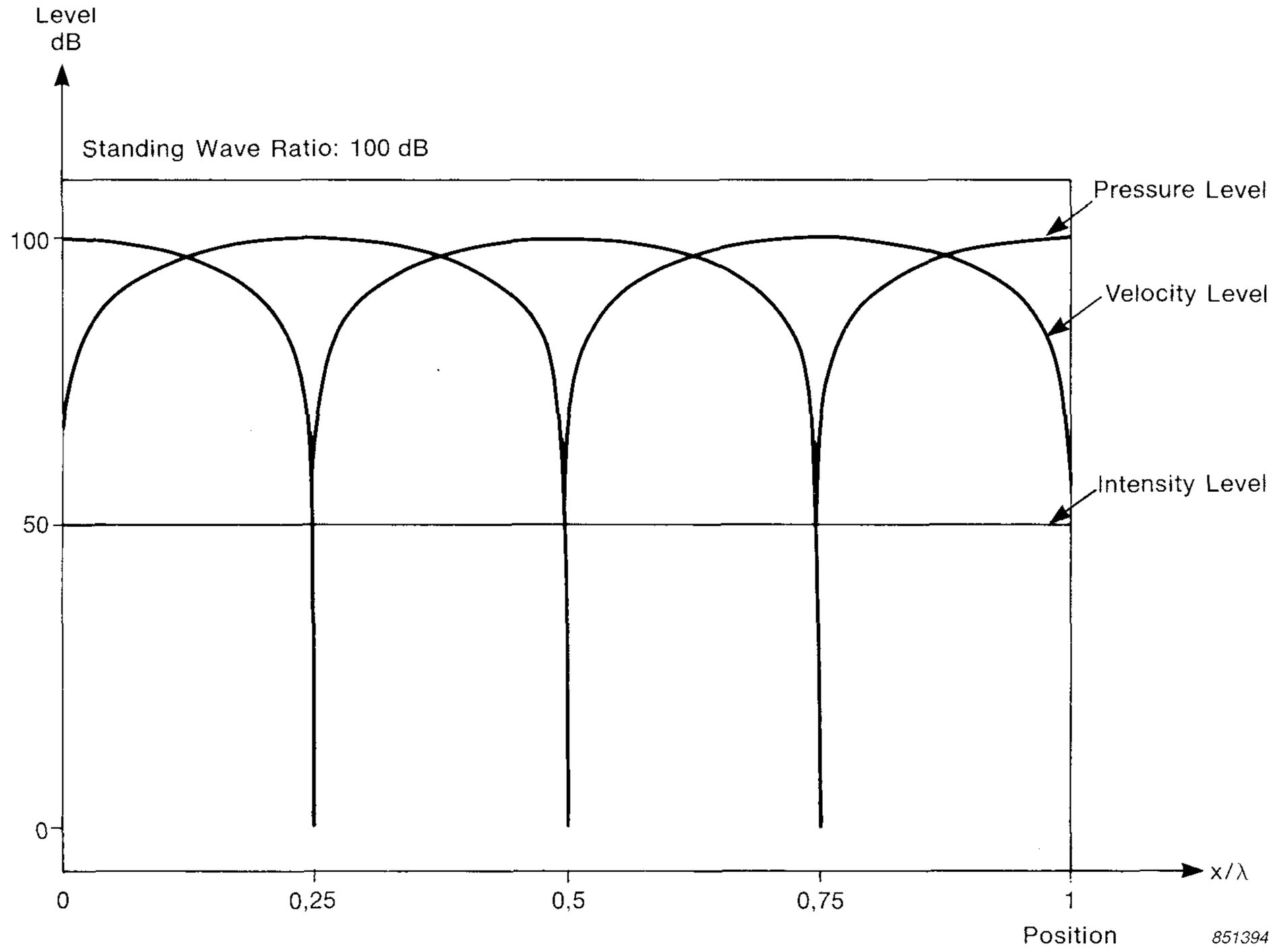

Fig. A.3. The level of pressure, Intensity and velocity for a standing wave, where the standing wave ratio is 100 dB. One wavelength is shown

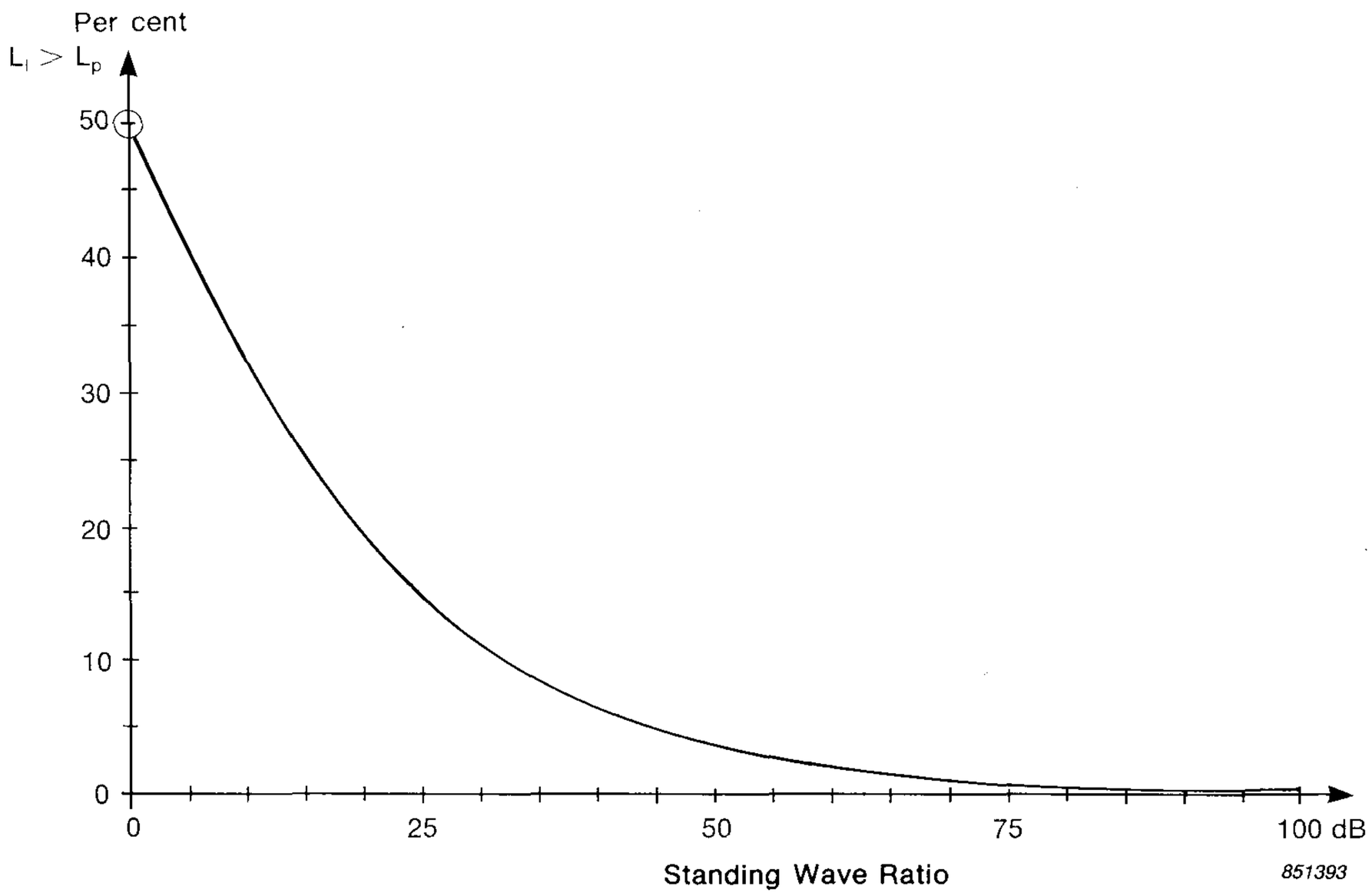

Fig. A.4. The relative amount of positions in a standing wave, where the Intensity level is higher than the pressure level, that is $L_K > 0$ dB

APPENDIX B

Error due to Phase Mismatch

If we consider the Residual Intensity level as being the system noise for our measurements, and that the measured intensity level as being the signal contaminated by the system noise, we have

$$L_I : Signal \pm Noise \tag{B.1}$$

$$L_{I,R} : Noise \tag{B.2}$$

where L_I and $L_{I,R}$ are measured quantities. If instead of using $1\,pW/m^2$ and $20\,\mu Pa$ ($L_I = 0$ dB and $L_p = 0$ dB) as our references use the pressure levels $L_{p,R}$ and L_p as indicated in Fig.B.1 we have

$$L_K : Signal \pm Noise \tag{B.3}$$

$$L_{K,0} : Noise \tag{B.4}$$

The relative amount of error due to system noise can be defined as

$$L_{\epsilon,p} = 10 \log \left[\frac{I_{measured}}{I_{true}}\right] \tag{B.5}$$

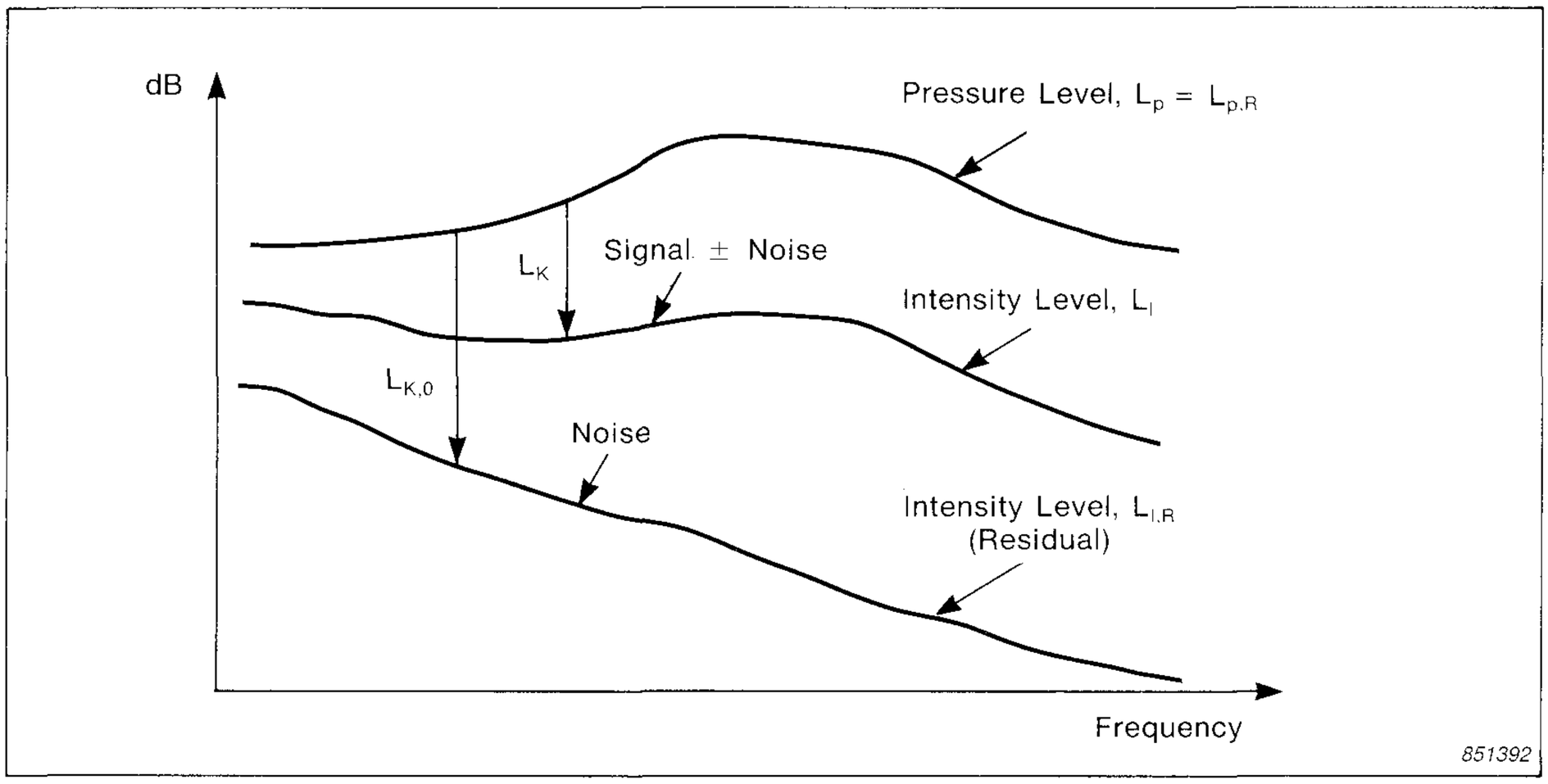

Fig. B.1. Signal to system noise ratio for Intensity measurements

Combining eqs. (B.3), (B.4) and (B.5) we get

$$L_{\epsilon,p} = 10 \log \left(\frac{10^{L_K/10}}{10^{L_K/10} \mp 10^{L_{K,0}/10}} \right)$$

$$= 10 \log \left(\frac{1}{1 \mp 10^{(L_{K,0} - L_K)/10}} \right)$$

$$= -10 \log \left(1 \mp 10^{(L_{K,0} - L_K)/10} \right) \qquad \text{(B.6)}$$

Equation eq. (B.6) is shown in Fig.B.2 for reactivity indices larger as well as smaller than the Residual Intensity index.

The upper right hand curve shows the case when

$$\text{sign } L_{I,\,measured} = \text{sign } L_{I,\,true} = \text{sign } L_{I,Residual}$$

When $L_{K,0} - L_K = -3\,\text{dB}$, we have that $L_{I,true} = L_{I,Residual}$, so that the measured intensity level, $L_{I,\,measured}$, will be 3 dB higher than the true intensity level. The error is a 3 dB overestimation.

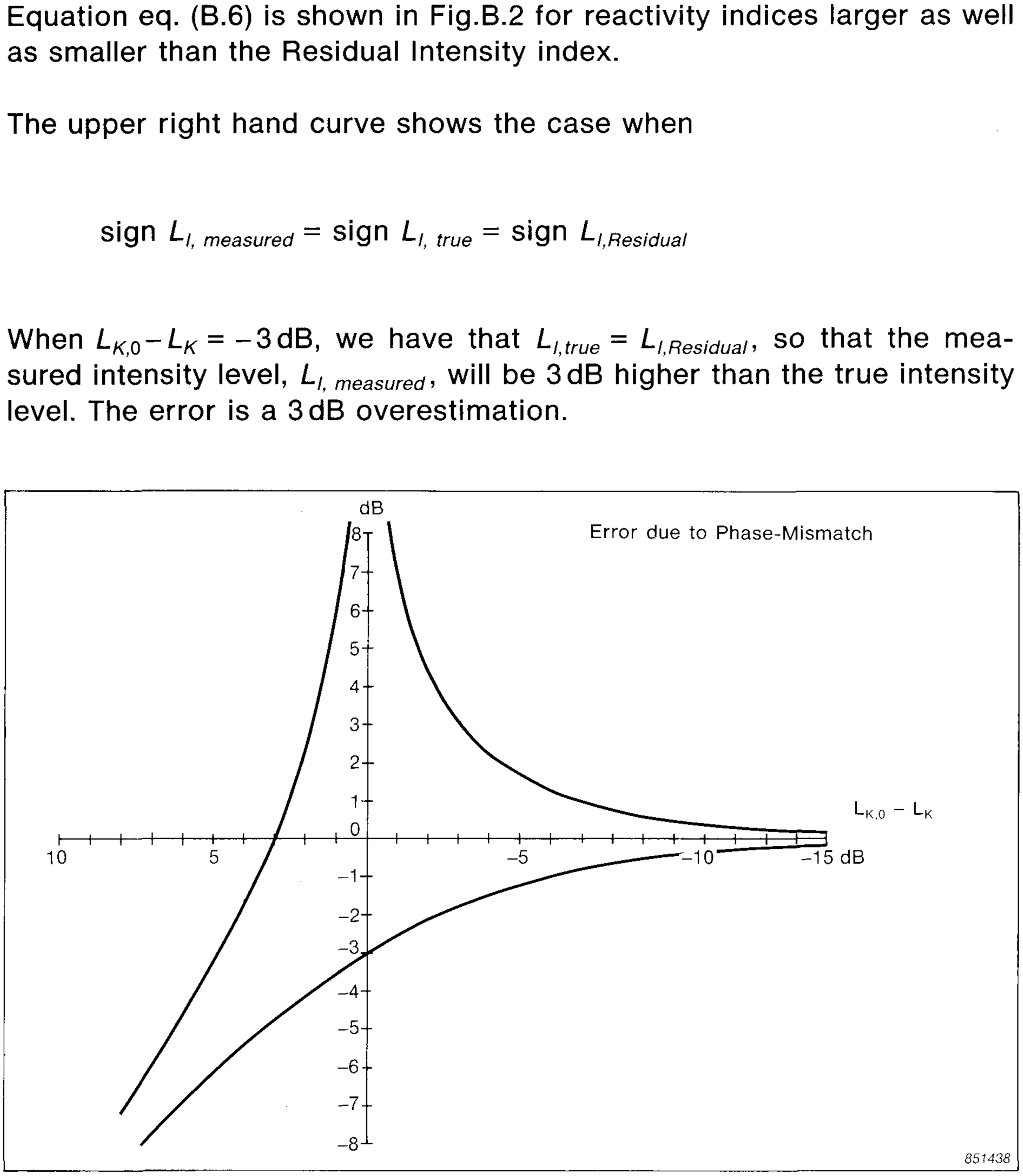

Fig. B.2. Error due to phase mismatch as a function of $L_{K,0} - L_K$

The lower curve shows the case when

$$\text{sign } L_{I,\,measured} = \text{sign } L_{I,\,true} \neq \text{sign } L_{I,\,Residual}.$$

In this case the intensity will always be underestimated.

When $L_{K,0} - L_K = 0\,\text{dB}$ and L_K and $L_{K,0}$ have opposite signs we have that $L_{I,\,true} = L_{I,\,measured} + 3\,\text{dB}$. This means that the intensity is underestimated by 3 dB.

$L_{K,0} - L_K = +\infty\,\text{dB}$ occurs when the true intensity level $L_{I,\,true}$ is equal to the Residual Intensity level $I_{I,R}$ but with opposite sign. In this case the measured intensity level $L_{I,measured} = -\infty\,\text{dB}$ and thus we have an infinitely high underestimation of the intensity.

The upper left hand curve shows the case when

$$\text{sign } L_{I,\,measured} \neq \text{sign } L_{I,\,true} \neq \text{sign } L_{I,\,Residual}$$

or

$$\text{sign } L_{I,\,true} \neq \text{sign } L_{I,\,measured} = \text{sign } L_{I,\,Residual}$$

Where $L_{K,0} - L_K = +\,3\,\text{dB}$ we have the case that the measured level $L_{I,\,measured}$ is equal to the true level of the signal $L_{I,\,true}$ but having the wrong sign.

When measuring in a sound field where the intensity is equal to zero, the two upper curves go towards infinity.

In this case the measured intensity will be the Residual Intensity of the analyzer $L_{I,R}$. Thus $L_{K,0} - L_K = 0\,\text{dB}$ and we have an infinitely high overestimation of the true intensity.

These curves are of course only of academic interest and should never be used for correction of measured intensity levels. On the other hand they indicate that the measured intensity level should always be at least 7 dB above the Residual Intensity level to ensure a correct sign and an accuracy in estimating the true intensity level better than $\pm$ 1 dB.

APPENDIX C

Random Error

From Refs.[7,10] we have that the variance of the imaginary part of the Cross-spectrum can be expressed as

$$\text{var}\,[\text{Im}\,G_{AB}] = \sigma^2\,[\text{Im}\,G_{AB}]$$

$$= \frac{1}{2BT}\,[G_{AA}\,G_{BB} + \text{Im}^2 G_{AB} - \text{Re}^2\,G_{AB}] \qquad \text{(C.1)}$$

where σ is the standard deviation of the quantity inside the brackets.

The intensity is calculated from the imaginary part of the cross-spectrum as shown in equation (C.2).

$$I = -\frac{\text{Im}\,G_{AB}}{\rho\omega\Delta r} \qquad \text{(C.2)}$$

Now we have $$\sigma\,[I] = \sigma\,[\text{Im}\,G_{AB}]/\rho\,\omega\,\Delta r \qquad \text{(C.3)}$$

and $$\sigma^2\,[I] = (\sigma[\text{Im}\,G_{AB}]/\rho\,\omega\Delta r)^2 = \frac{\sigma^2\,[\text{Im}\,G_{AB}]}{(\rho\,\omega\Delta\,r)^2} \qquad \text{(C.4)}$$

The relative random error is defined as

$$\epsilon_r\,[I] = \frac{\sigma\,[I]}{I} \qquad \text{(C.5)}$$

Combining eqs. (C.1), (C.2), (C.4), and (C.5) gives

$$\epsilon_r^2\,[I] = \frac{\sigma^2\,[\text{Im}\,G_{AB}]}{\text{Im}^2\,G_{AB}}$$

$$= \frac{1}{2BT}\left[\frac{G_{AA}\cdot\,G_{BB} + \text{Im}^2\,G_{AB} - \text{Re}^2\,G_{AB}}{\text{Im}^2\,G_{AB}}\right] \qquad \text{(C.6)}$$

Inserting $G_{AA} \cdot G_{BB} = (\mathrm{Re}^2 G_{AB} + \mathrm{Im}^2 G_{AB})/\gamma^2$

where γ^2 is the coherence function, we get

$$\epsilon_r^2[I] = \frac{1}{2BT}\left[\frac{\mathrm{Re}^2\ G_{AB} + \mathrm{Im}^2\ G_{AB}}{\gamma^2\ \mathrm{Im}^2\ G_{AB}} + \frac{\mathrm{Im}^2\ G_{AB}}{\mathrm{Im}^2\ G_{AB}} - \frac{\mathrm{Re}^2\ G_{AB}}{\mathrm{Im}^2\ G_{AB}}\right]$$

$$= \frac{1}{2BT}\left[\frac{\cot^2\Phi}{\gamma^2} + \frac{1}{\gamma^2} + 1 - \cot^2\Phi\right]$$

$$= \frac{1}{2BT}\left[1 + \frac{1}{\gamma^2} + \frac{(1-\gamma^2)\cot^2\Phi}{\gamma^2}\right] \qquad \text{(C.7)}$$

using $\cot^2\Phi = \dfrac{1-\sin^2\Phi}{\sin^2\Phi}$ we have

$$\epsilon_r^2[I] = \frac{1}{2BT}\left[\ 1 + \frac{1}{\gamma^2} + \frac{(1-\gamma^2)\,(1-\sin^2\ \Phi)}{\gamma^2\ \sin^2\Phi}\right]$$

$$= \frac{1}{BT}\left[1 + \frac{(1-\gamma^2)}{2\ \gamma^2\ \sin^2\Phi}\right] \qquad \text{(C.8)}$$

The normalized random error is a function of the BT product, the calculated coherence and the calculated phase difference between the two channels including signals and measuring chains. It should be noted that Seybert [11] has evaluated an equivalent formula

$$\epsilon_r^2[I] = \frac{1}{BT}\left[\frac{1}{\gamma^2} + \frac{(1-\gamma^2)\cot^2\ \Phi}{2\gamma^2}\right] \qquad \text{(C.9)}$$

under the assumption that the phase angle Φ is small.

The formula eq. (C.8) is a more general formula since it is not evaluated under this assumption.

INFLUENCE OF TRIPODS AND MICROPHONE CLIPS ON THE FREQUENCY RESPONSE OF MICROPHONES

by

K. Zaveri, M.Phil.

ABSTRACT

Use of microphone clips and tripods to support microphones causes disturbance of the sound field and thus causes errors in sound level measurements. This article illustrates the amount of errors introduced for different mounting configurations, and shows how these errors can be kept to a minimum.

SOMMAIRE

Les pinces et les trépieds utilisés pour maintenir les microphones provoquent des perturbations du champ sonore qui peuvent fausser les mesures du niveau sonore. Cet article illustre l'amplitude des erreurs provoquées par les différents types de montage, et montre comment ramener ces erreurs à un minimum.

ZUSAMMENFASSUNG

Mikrofonhalter und Stative verursachen Störungen im Schallfeld und beeinflussen somit die Schallmessung. In diesem Artikel wird der sich für verschiedene Aufbauten ergebende Fehler diskutiert und gezeigt, wie sich diese Fehler auf ein Minimum reduzieren lassen.

Introduction

A free-field equalized microphone measures the sound pressure existing at the position of the diaphragm in the absence of the microphone, thus compensating for the interference created in the sound field due to the microphone itself. If a microphone clip, extension rods and tripod are used to support the microphone, however, disturbance of the sound field can be caused, especially if the latter is mounted close to the microphone [1]. To investigate the amount of error introduced, measurements were carried out in an Anechoic Chamber, using a small loudspeaker, and a 1/2″ free field Microphone Type 4133 suspended by thin strings from metal wires. Their relative positions in the Anechoic Chamber are shown in the sketch of Fig.1.

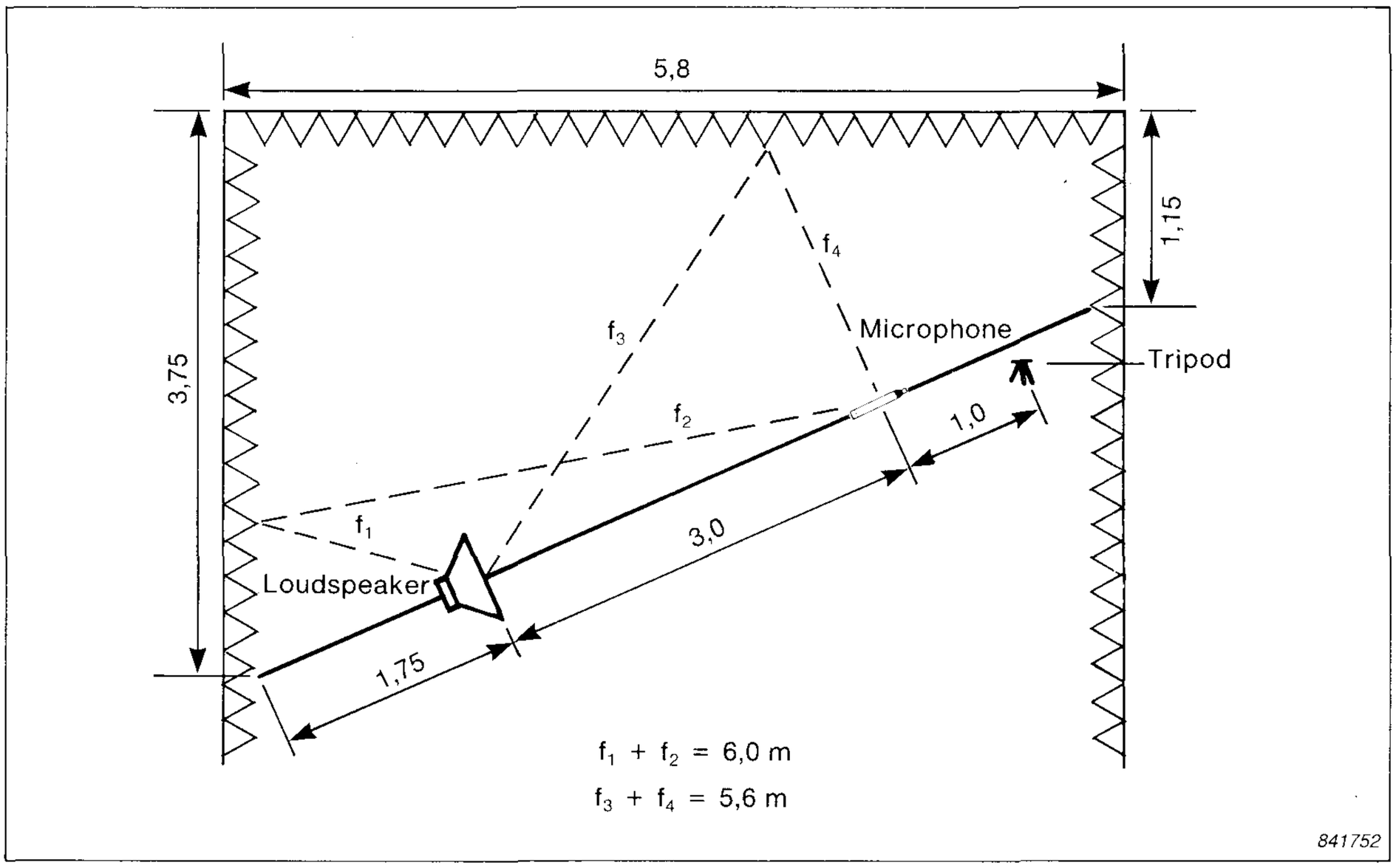

Fig.1 Microphone, Tripod and loudspeaker positions in the Anechoic Chamber

The record length in the Narrow Band Analyzer 2031 corresponding to full scale frequency range of 20 kHz is 20 ms. As the "after trigger recording" was set to 0,4, reflected signals from objects at a distance of $(344 \times 0{,}4 \times 20 \times 10^{-3})/2 = 1{,}38$ m would be recorded. Thus signals reflected from the tripod wil be recorded whilst most of those reflected from the walls will be subdued

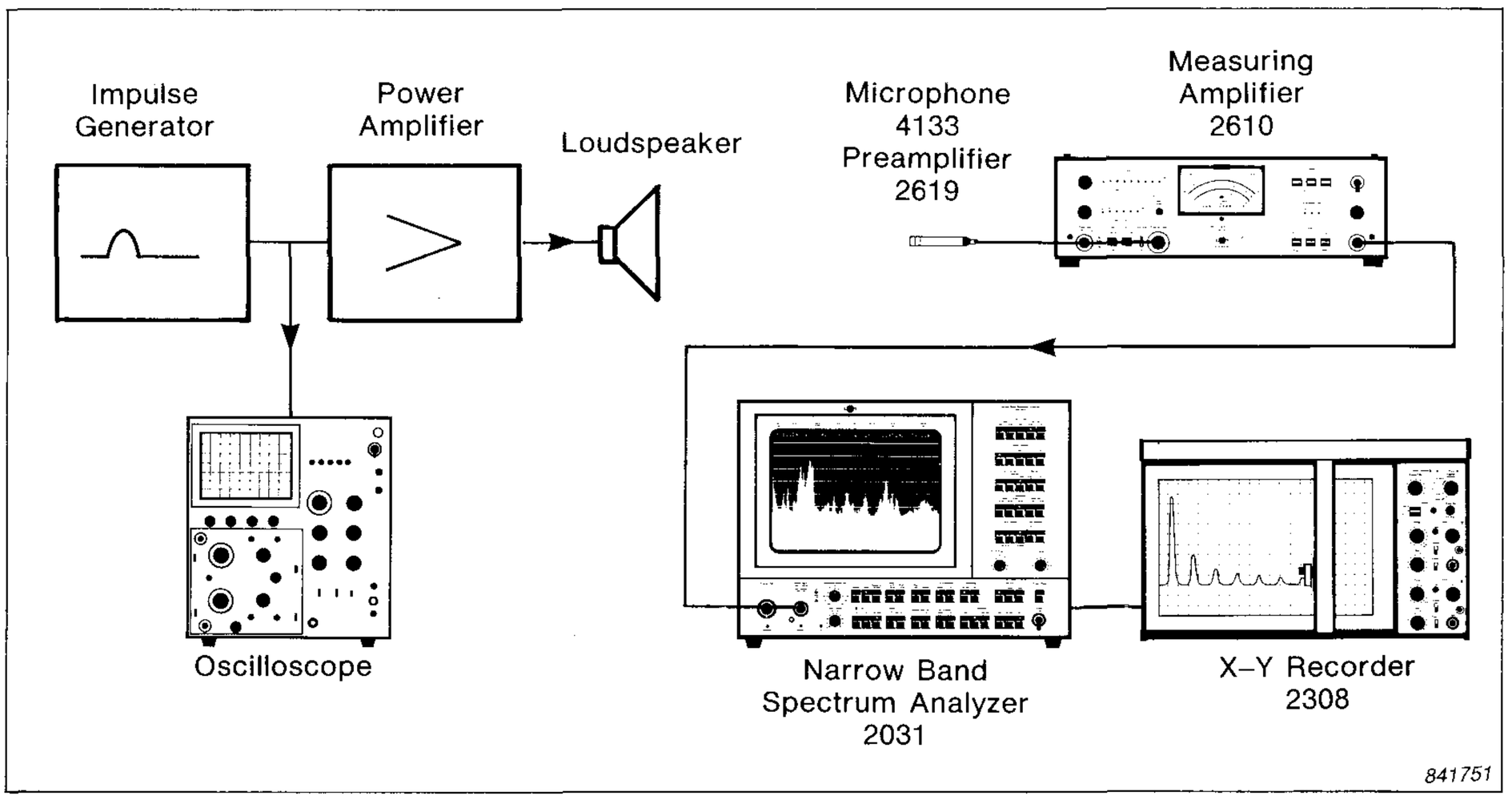

Fig.2. Measuring instrumentation set-up

Measurement Procedure

The instrumentation set-up used is shown in Fig.2. As a test signal an impulse was transmitted via the loudspeaker, and analysed using a Narrow Band Spectrum Analyzer Type 2031. The frequency response obtained is shown in Fig.3a. The rather heavy ripples in the frequency range above 6 kHz, as seen in the figure, were found to persist when the analysis was repeated. It was found to be caused by sound reflections from the wire mesh constituting the floor. Covering the wire mesh with rockwool and repeating the measurements gave a response curve as illustrated in Fig.3b. The ripples can be seen to be significantly reduced. This spectrum was stored in the memory of the analyzer as a reference. As there is not enough energy in the impulse below 500 Hz, measurement results in this article are not valid below this frequency.

A microphone clip UA 0588 with its swing arm in the horizontal position was now mounted on the microphone. To examine the influence of sound reflections from the clip, the impulse signal was again analyzed and the reference spectrum was subtracted from it. The difference in dB is shown in Fig.4a. A similar curve was also obtained with the swing arm in the vertical position, and is illustrated in Fig.4b. As expected, the disturbance caused by the swing arm in the vertical position is higher

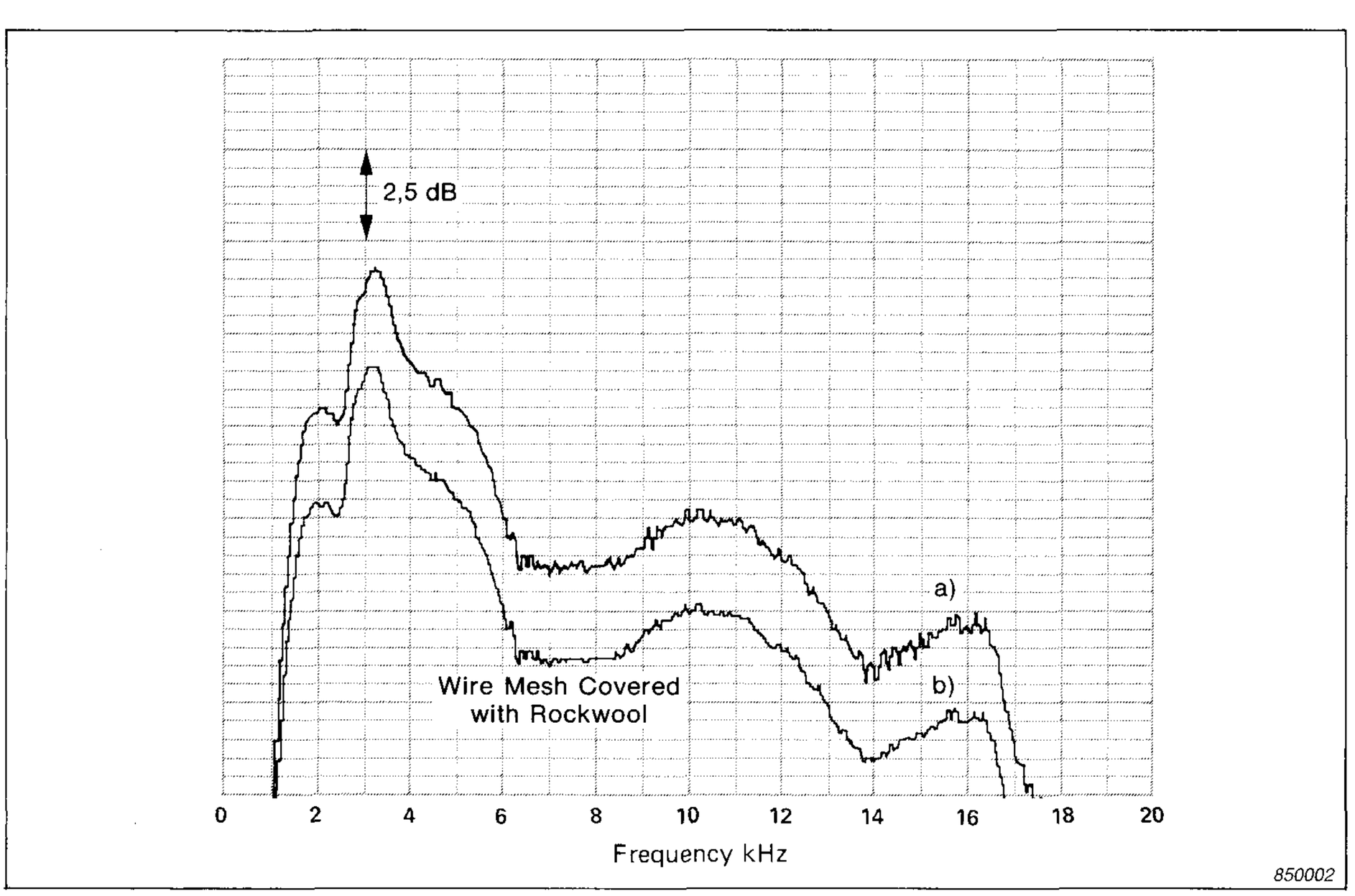

Fig.3. Frequency response of impulse
a. with bare wire mesh
b. with wire mesh covered with rockwool

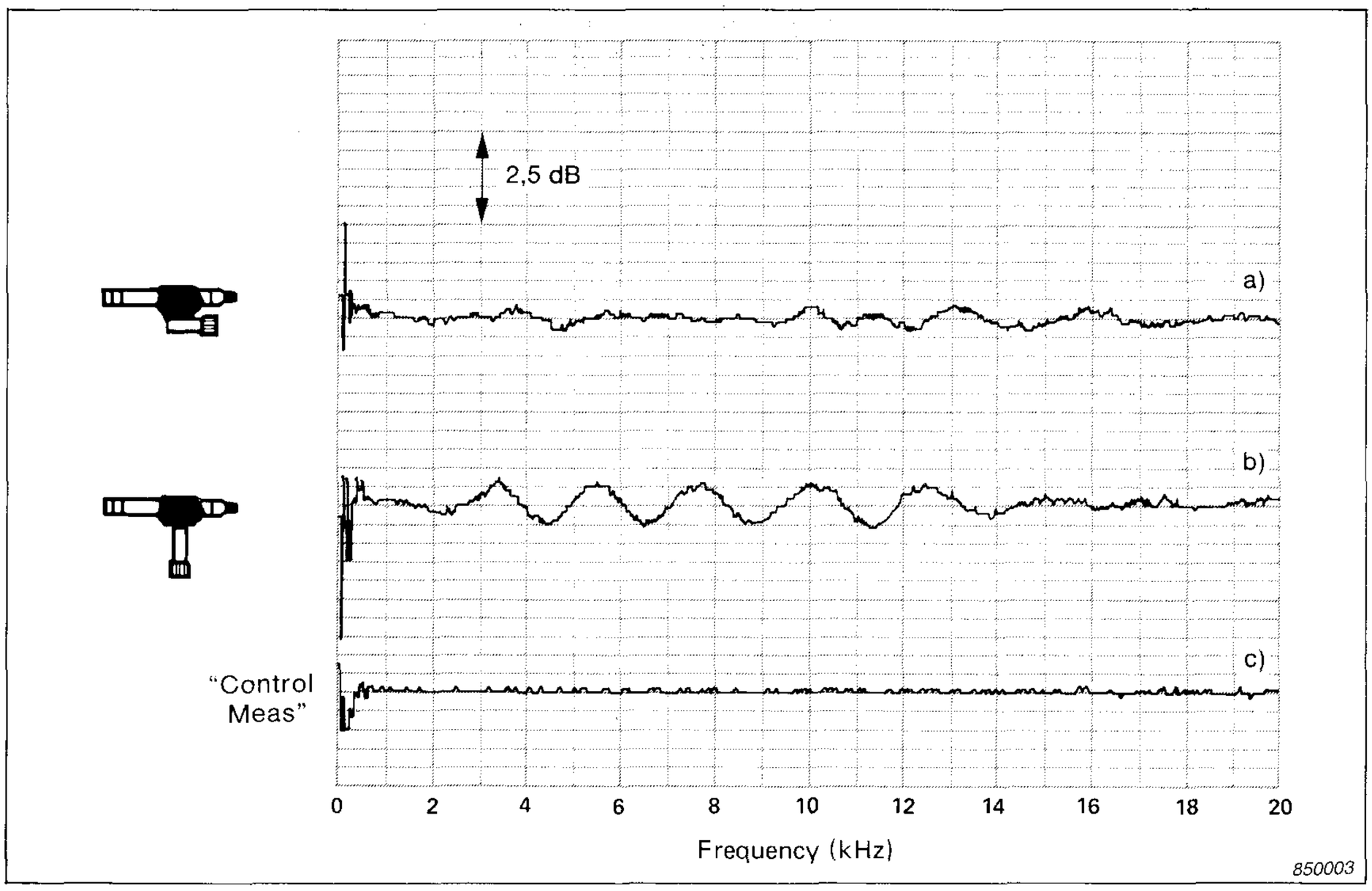

Fig.4. Errors caused by microphone clip with swing arm
a. in horizontal position
b. in vertical position
c. "Control Meas"

and of the order of ± 0,5 dB. To ensure that this was caused exclusively by the microphone clip, the experiment was repeated without the clip, and the spectrum subtracted from the reference spectrum. The result is shown in Fig.4c, and the difference is seen to be less than ± 0,2 dB. In the following, such a control measurement was taken after each of the interfering objects was removed, and the curves are indicated by "Control Meas" on the figures.

To investigate the effects of connecting the extension rods of the tripod UA 0587 to the microphone clip, similar measurements were carried out. Figs.5a, b, c, and d, show the interference caused by the microphone clip and when the extension rods are connected at 0°, 30°, 60° and 90° from the horizontal. Again the largest interference is caused for the 90° case, however, the error is not greater than ± 0,5 dB. In Fig.5d the peaks and valleys are shifted in frequency relative to those in Fig.4b, however, the magnitude of the error is still of the order of ± 0,5 dB. Fig.5e illustrates the "Control Meas".

Oftentimes in literature, the microphone is seen to be mounted directly on top of the ball-joint of the microphone tripod. The errors caused by

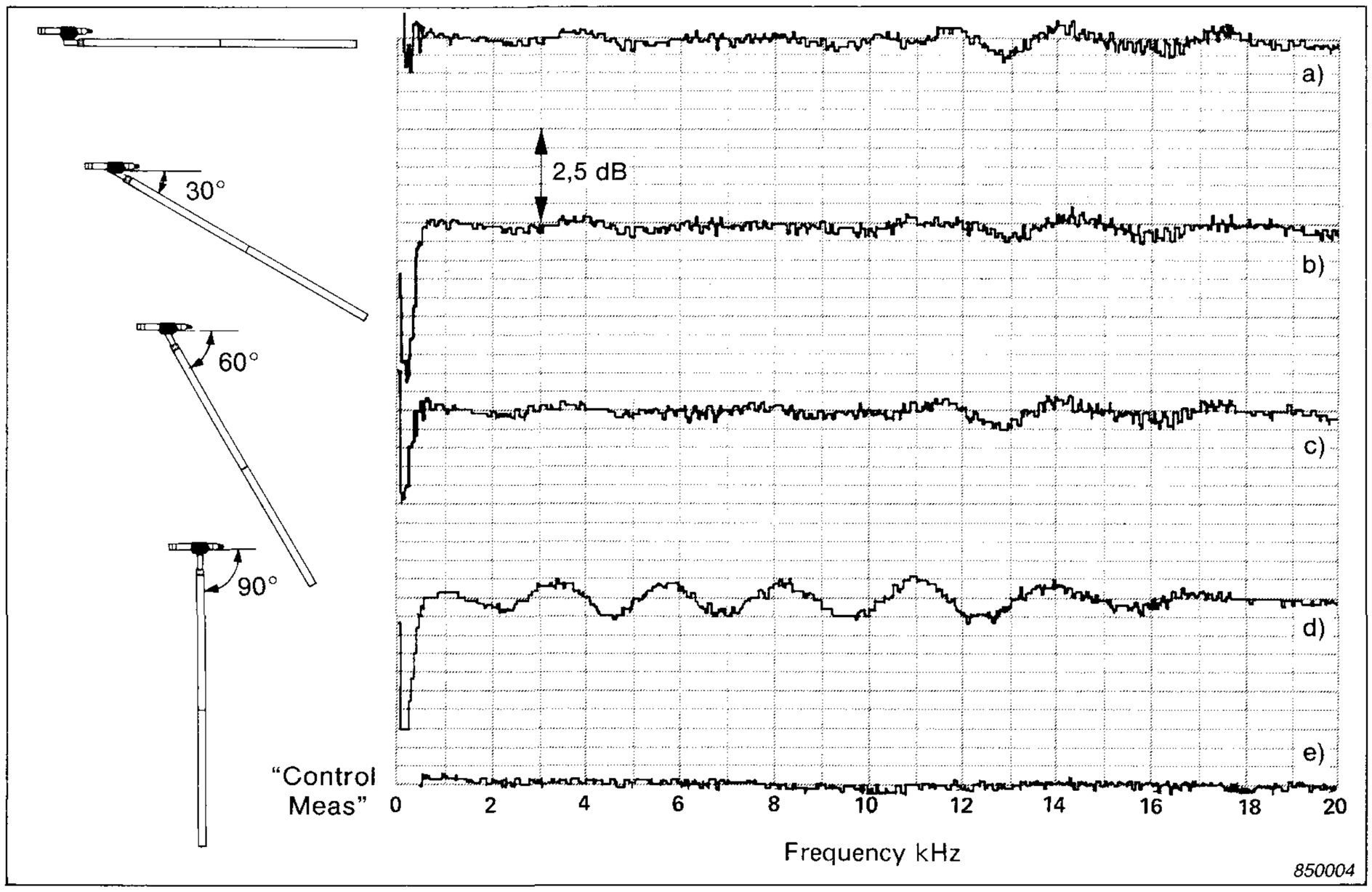

Fig.5. Errors caused by microphone clip and two-piece extension rod connected at

a. 0° from the horizontal
b. 30° from the horizontal
c. 60° from the horizontal
d. 90° from the horizontal
e. "Control Meas."

this form of mounting are illustrated in Fig.6a, whereas Fig.6b shows results for the same conditions but with the tripod as well. The difference between Fig.6a and Fig.6b is not significant, indicating the influence of the microphone tripod to be negligible. However, the error due to the ball-joint is increased to ± 1,3 dB.

As one would expect, this interference is removed when the microphone is mounted on the two-piece extension rod fixed to the tripod, as can be seen in Fig.6c. The errors caused here are less than ± 0,5 dB, similar to those of Figs.5a, b, and c, as long as the angles between the horizontal microphone and the extension rod is 60° or less.

To further improve the results of Fig.5a, (i.e. to minimize the reflections from the microphone clip being mounted so close to the microphone), the flexible extension rod UA 0196 was made use of. The results are shown in Figs.7a, b, and c for 0°, 60°, and 90° between the microphone

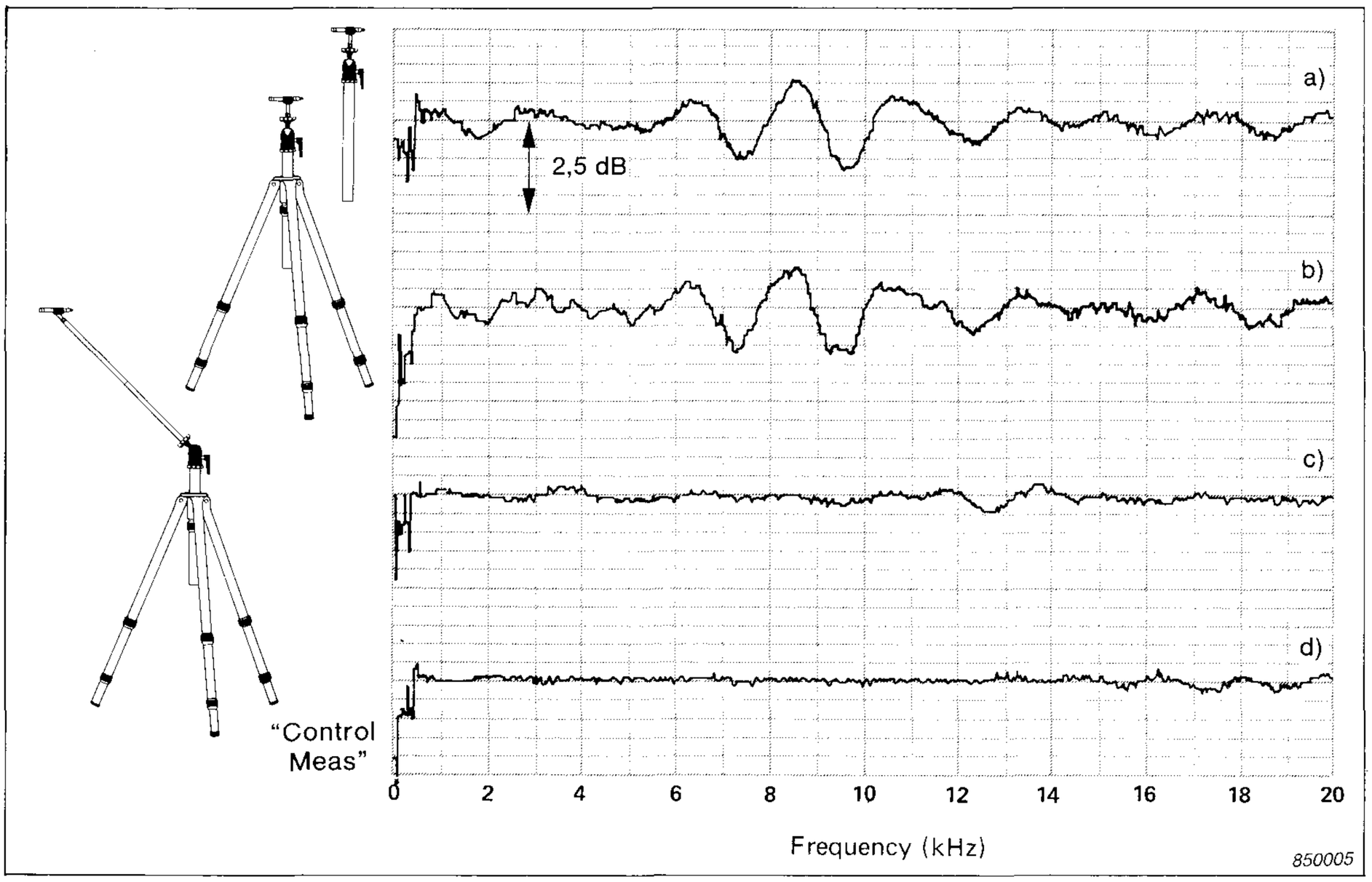

Fig.6. Errors caused by microphone clip when
a. mounted directly on ball-joint
b. mounted directly on ball-joint together with the tripod
c. mounted to tripod with the two-piece extension rod
d. "Control Meas"

and the two-piece extension rod. It can be seen that the errors are reduced to ± 0,2 dB for angles less than 60° and to ± 0,5 dB for 90°. The use of the flexible extension rod is probably even more imperative in conjunction with the pressure microphone, when it is used in a free field, and has therefore to be mounted at 90° incidence. Fig.8b shows the reduction in error achievable with the flexible extension rod compared with Fig.8a where the microphone clip is mounted close to the microphone.

Finally, Fig.9 shows the results obtained with an 1″ Microphone Type 4145 with the microphone clip UA 0802 and the two-piece extension rod mounted at 90° from the horizontal microphone. Compared to the results of Fig.5d for the 1/2″ microphone, the error is significantly lower, approximately ± 0,3 dB. This is because the 1″ microphone is considerably less sensitive than 1/2″ microphones to reflections coming from behind the microphone as can be seen from Figs.10a and b.

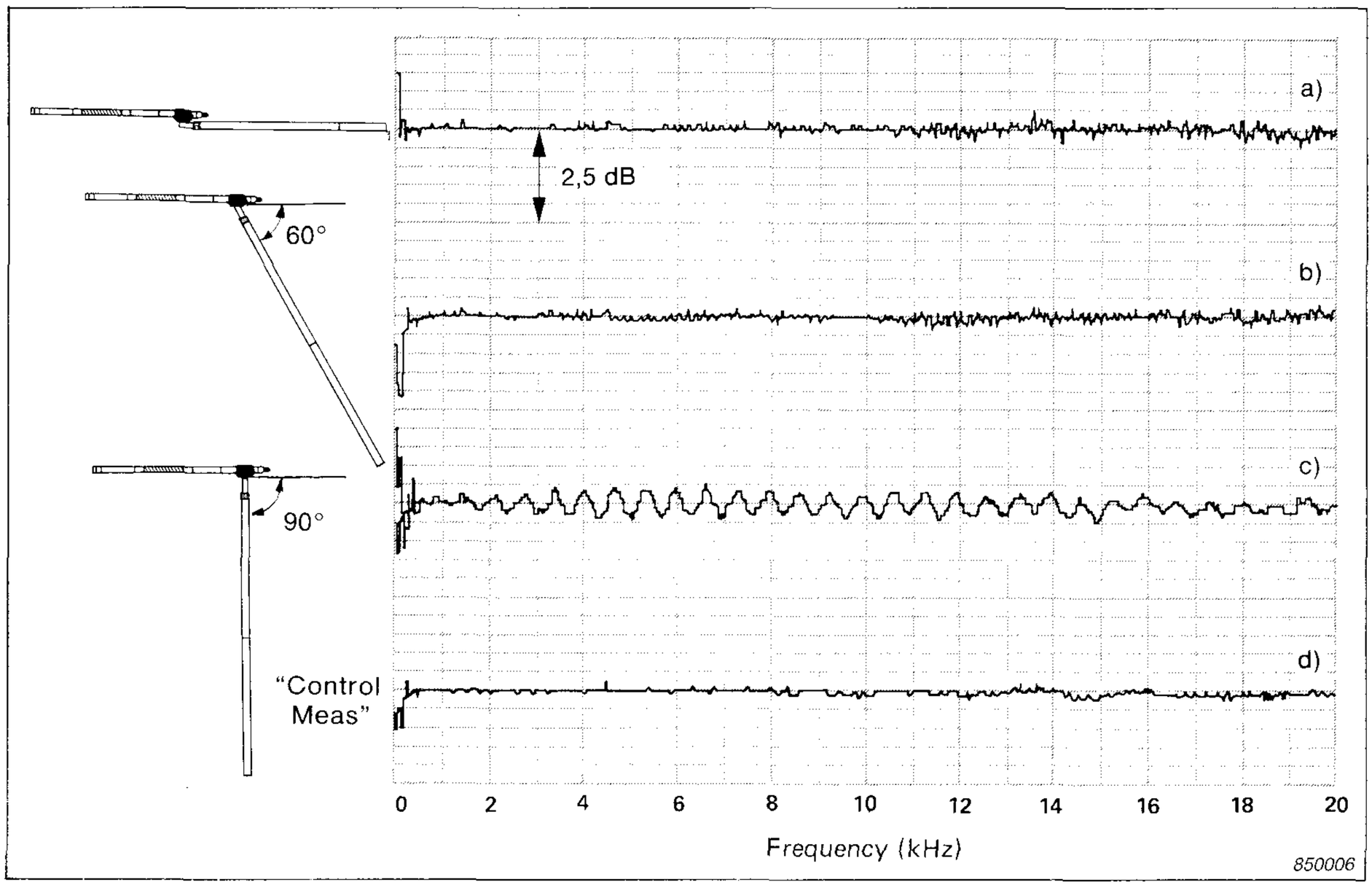

Fig.7. Errors caused using a flexible extension rod and the two-piece extension rod at
a. 0° from the horizontal
b. 60° from the horizontal
c. 90° from the horizontal
d. "Control Meas"

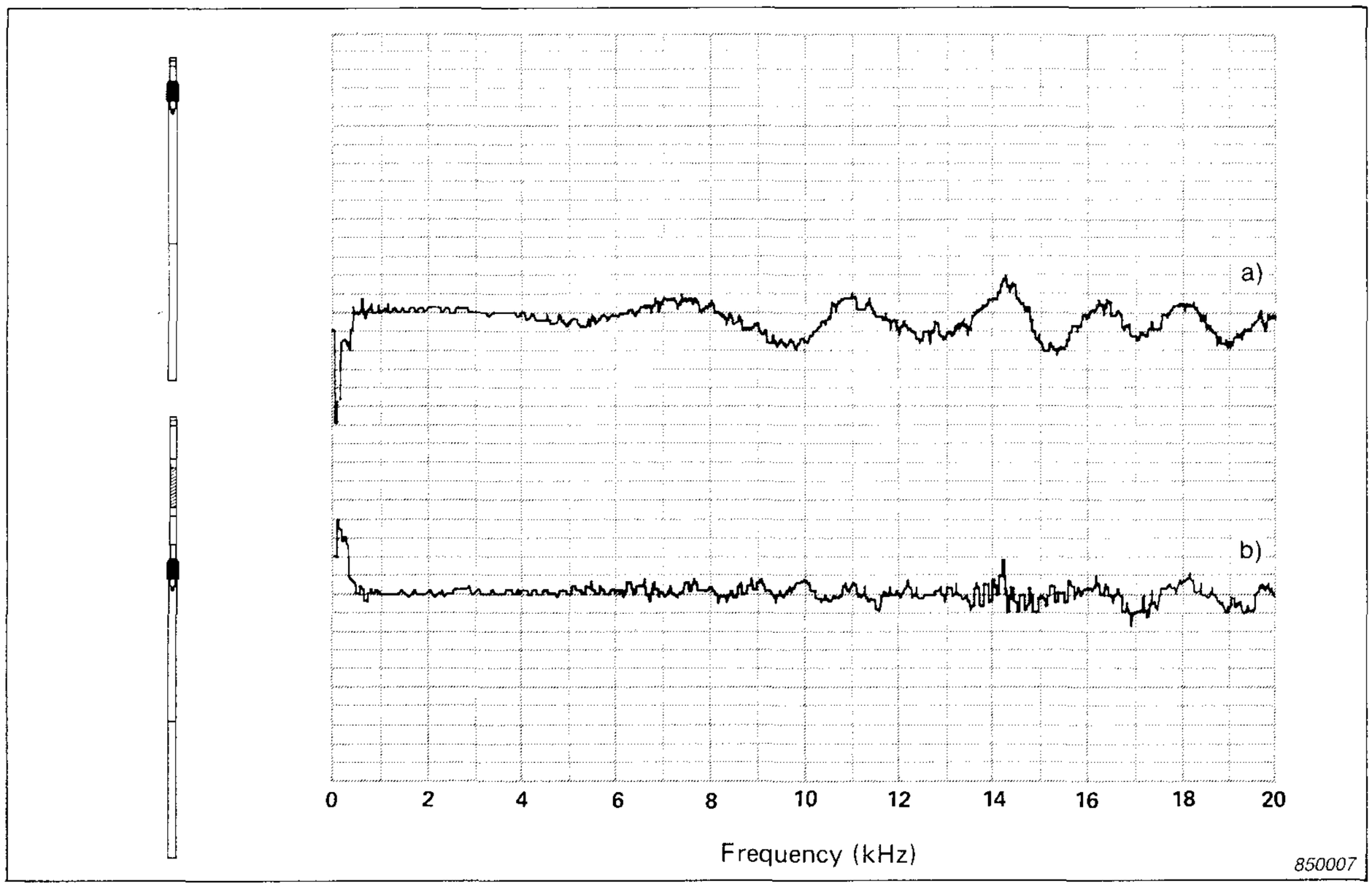

Fig.8. Errors caused for 90° sound incidence by the microphone clip when it is used
a. without the flexible extension rod
b. with the flexible extension rod

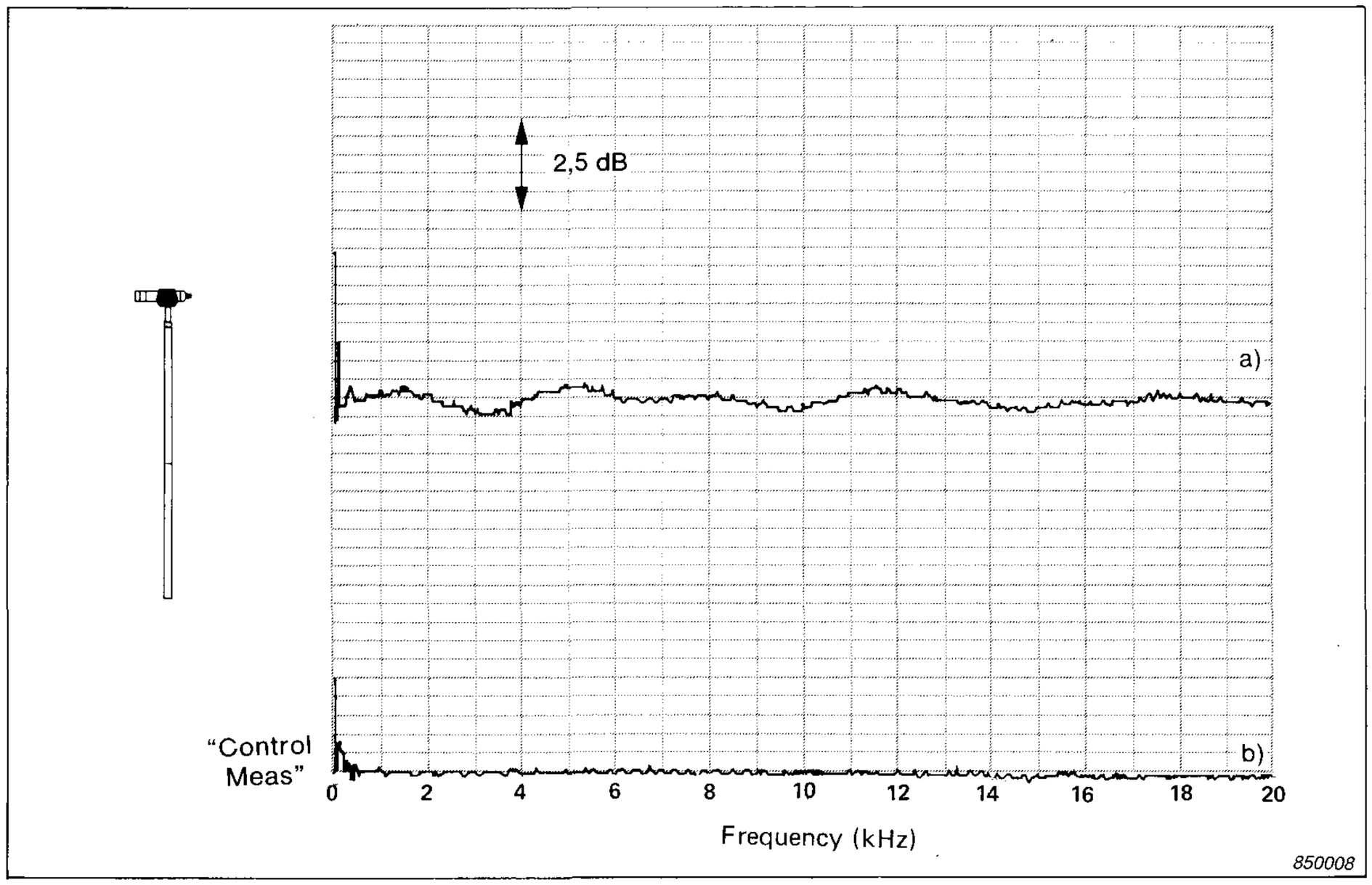

Fig.9.a Errors caused by microphone clip for a 1″ microphone with the two-piece extension rod at 90° from the horizontal
b. "Control Meas"

Conclusions

From the results it is obvious that mounting of the microphone directly on the tripod should be avoided. To keep errors within ± 0,5 dB, the two-piece extension rod should be made use of, and should be mounted preferably less than 60° from the horizontal. For the same configuration, the error can be reduced further down to ± 0,2 dB by inserting the flexible extension rod between the microphone and the preamplifiers on which the microphone clip is mounted. One inch microphones are considerably less sensitive to clips and tripods than 1/2″ microphones.

It should be noted that results obtained in this article using narrow band analysis can be considered to be the worst cases, such as obtained when dealing with pure tones or very narrow bands of noise. In practice, where broad band noise is emitted and measurements carried out in 1/3 octaves, which is very often the case, considerably lower errors will occur on account of averaging in the relatively broader bandwidths.

Acknowledgements
The author wishes to thank Peter Møller for his assistance with the measurements.

References

[1] ZOLLNER, M. "Einfluß von Stativen und Halterungen auf den Mikrofonfrequenzgang, *Acoustica*, Vol.51 (1982), pp.268–272

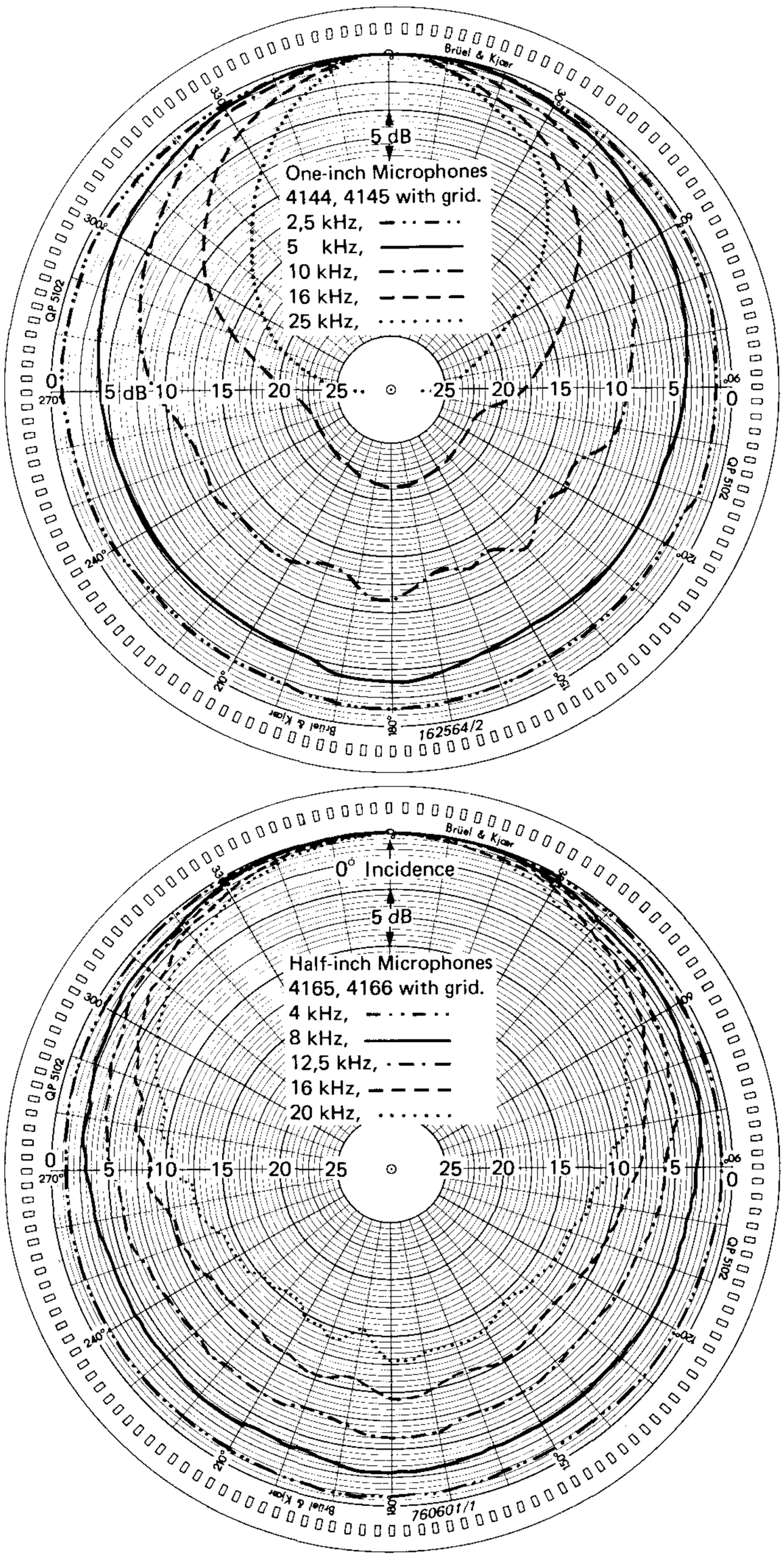

Fig.10. Directional Characteristics for
a. 1″ microphones
b. 1/2″ microphones

News from the factory

Portable Machine Vibration Analyzer Type 2515

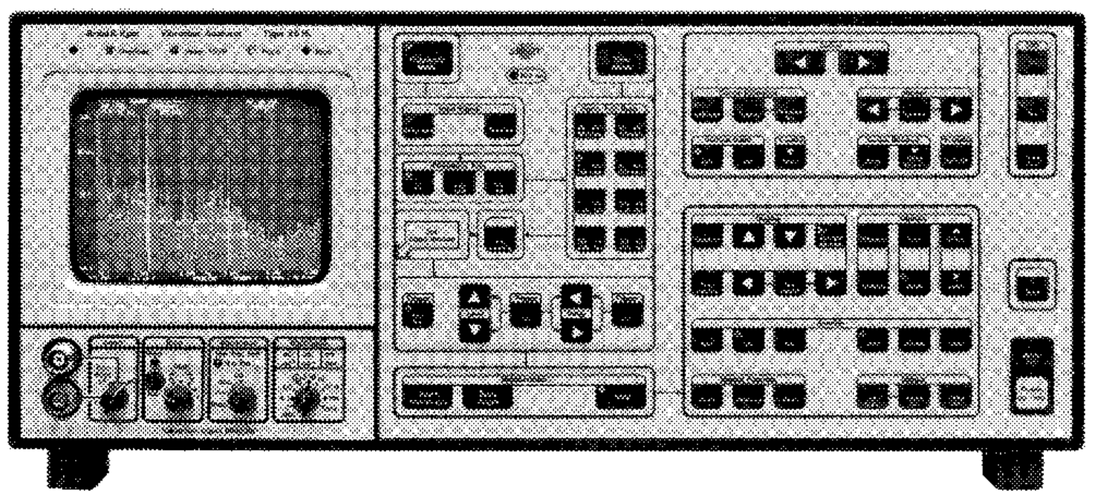

Brüel & Kjær's Type 2515 is a portable battery-powered FFT analyzer designed for the requirements of everyday machine monitoring. The solidly built single-channel analyzer has waterproof and dust-proof characteristics better than IP 44 in accordance with IEC 529. A large non-volatile memory holds up to 100 constant percentage bandwidth spectra or 50 constant bandwidth spectra, cepstra or time records, along with the pushbutton settings used in the recording. When a recording is recalled and displayed, the original pushbutton settings are also reactivated.

With its clearly laid-out front panel, the Type 2515 is easy to operate and makes day-to-day monitoring a straightforward matter. Newly measured spectra are easily compared with reference spectra. The built-in charge preamplifier allows accelerometers to be connected directly, and the 2515 also incorporates Brüel & Kjær's unique speed compensation technique.

The Analyzer incorporates a wide range of facilities for troubleshooting vibration problems, including cepstrum, non-destructive zoom, harmonic cursor with fine tuning, reference cursor, phase read out, computation of overall vibration levels, advanced triggering facilities, external sampling, scan analysis, exponential averaging, time averaging, expanded time

function, and a choice of weightings for continuous or transient signals. The fully annotated display axes can be set to log. or lin. scales, and the operator can select metric, British/American or engineering units, or dB's.

The IEEE–488 interface allows the analyzer to be connected to further post-processing instruments for trend analysis, data management and storage/retrieval of reference spectra. Hard copy can also be obtained using either the analogue or video outputs. The Type 2515 can be supplied in a reinforced leather case with shoulder strap and comes complete with a mains supply adaptor/battery charger.

Field Balancing Set Type 3537

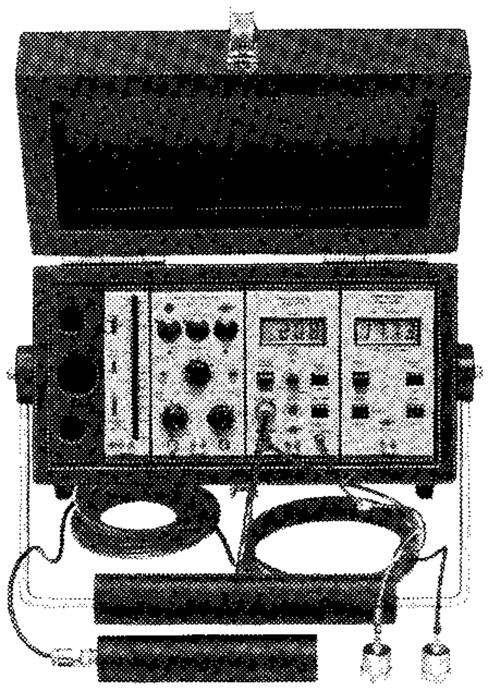

The portable Field Balancing Set, Type 3537 a development of the earlier Type 9537, is a handy, battery operated system which combines all the measuring instruments needed for both single- and two-plane balancing of rigid rotors without dismounting them from their own bearings.

Measurement of the unbalance vibration is made via two Type 4370 Delta Shear® piezoelectric Accelerometers. Signal conditioning is carried out in a Charge Preamplifier, Type 2635 and the vibration level displayed on an Indicator Unit, Type 2433 which has a thermometer-type logarithmic display. The unbalance phase is displayed with a resolution of 1° on a Phase Indicator, Type 2976 with liquid crystal display. The phase reference is provided by an infra-red tachometer probe, which can operate at up to 800 mm from the rotor. Signal filtering is provided by a Tracking Filter, Type 1626 which tracks the rotation frequency

without prior tuning. Furthermore, Type 1626 has a sweep mode which enables frequency analyses of machine vibration to be performed.

The 3537 comes combined in a light-weight carrying-case together with battery chargers. Weighing only 10 kg, the Type 3537 is truly portable and ideal for field balancing applications.

Indicator Unit Type 2433

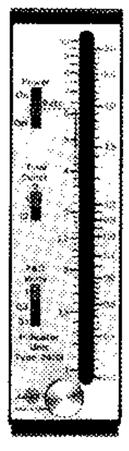

A new battery-operated AC voltmeter, the Indicator Unit Type 2433 is a development of an earlier model, the Type 5743, which has been available for some time on special order.

The Type 2433 uses a light emitting diode (LED) thermometer-type display composed of 41 LEDs enabling a 100 mm high-resolution scale to be accommodated in an instrument only 34,5 mm wide. Overrange, underrange, or a signal with too high a crest factor are shown by a flashing indicator. The Indicator Unit has three full-scale outputs of 1; 0,3 and 0,1 V, matching the outputs of a number of B&K instruments, and uses a logarithmic RMS detector that can accommodate the high crest factors often found in mechanical vibration signals. Two selectable time-constants, of 1 s and 10 s, enable measurement to be made of either deterministic or random signals with frequency components as low as 1 Hz.

The Type 2433 occupies 1/12 of the B&K standard rack width and can be incorporated with other B&K instruments in a variety of portable measuring systems built into a carrying-case. If the Indicator Unit is combined with a charge amplifier and any suitable piezoelectric accelerometer a versatile vibration meter results. Adding a tracking filter and phase indicator produces a portable balancing set.

Tracking Filter Type 1626

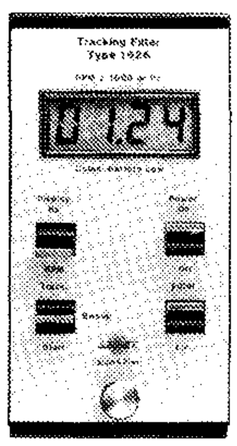

The battery-operated Tracking Filter Type 1626 (a development of the earlier Type 5856 which has been available on special order for some years) is specifically designed for field balancing of rigid rotors and vibration analysis when used with other suitable instruments from B & K.

The Type 1626 contains a highly selective band-pass filter which automatically tracks the rotation frequency of the rotor to be balanced, preventing unwanted vibrations from interfering with the measurements. The Tracking Filter has three fixed bandwidths of 0,1; 1 and 10 Hz, automatically selected as a function of the tracking frequency. The automatic bandwidth selection can be partly or fully disabled, giving down to 0,1 Hz bandwidth over the full frequency range. Display of the rotation frequency is given in either Hz or RPM on a large liquid-crystal display. For frequency analysis of machine vibration the Type 1626 has a sweep mode which can sweep the filters through a frequency range of 2 Hz to 2 kHz.

The other instruments normally required for field balancing together with the Type 1626, namely two accelerometers, a preamplifier, a voltmeter, a phase indicator and a tachometer probe, are all available from B & K and together can be installed in a carrying case to form a versatile portable balancing set and vibration analyzer. For frequency analysis the Type 1626 can tune a level recorder to synchronize the motion of the preprinted paper to give a hard-copy of the frequency spectrum.

PREVIOUSLY ISSUED NUMBERS OF BRÜEL & KJÆR TECHNICAL REVIEW

(Continued from cover page 2)

4-1979 Prepolarized Condenser Microphones for Measurement Purposes.
Impulse Analysis using a Real-Time Digital Filter Analyzer.
3-1979 The Rationale of Dynamic Balancing by Vibration Measurements.
Interfacing Level Recorder Type 2306 to a Digital Computer.
2-1979 Acoustic Emission.
1-1979 The Discrete Fourier Transform and FFT Analyzers.
4-1978 Reverberation Process at Low Frequencies.
3-1978 The Enigma of Sound Power Measurements at Low Frequencies.
2-1978 The Application of the Narrow Band Spectrum Analyzer Type 2031 to the Analysis of Transient and Cyclic Phenomena.
Measurement of Effective Bandwidth of Filters.
1-1978 Digital Filters and FFT Technique in Real-time Analysis.
4-1977 General Accuracy of Sound Level Meter Measurements.
Low Impedance Microphone Calibrator and its Advantages.
3-1977 Condenser Microphones used as Sound Sources.
2-1977 Automated Measurements of Reverberation Time using the Digital Frequency Analyzer Type 2131.
Measurement of Elastic Modulus and Loss Factor of PVC at High Frequencies.

SPECIAL TECHNICAL LITERATURE

As shown on the back cover page, Brüel & Kjær publish a variety of technical literature which can be obtained from your local B & K representative.
The following literature is presently available:

Mechanical Vibration and Shock Measurements (English), 2nd edition
Acoustic Noise Measurements (English), 3rd edition
Architectural Acoustics (English)
Strain Measurements (English, German)
Frequency Analysis (English)
Electroacoustic Measurements (English, German, French, Spanish)
Catalogs (several languages)
Product Data Sheets (English, German, French, Russian)

Furthermore, back copies of the Technical Review can be supplied as shown in the list above. Older issues may be obtained provided they are still in stock.

Printed in Denmark by Nærum Offset

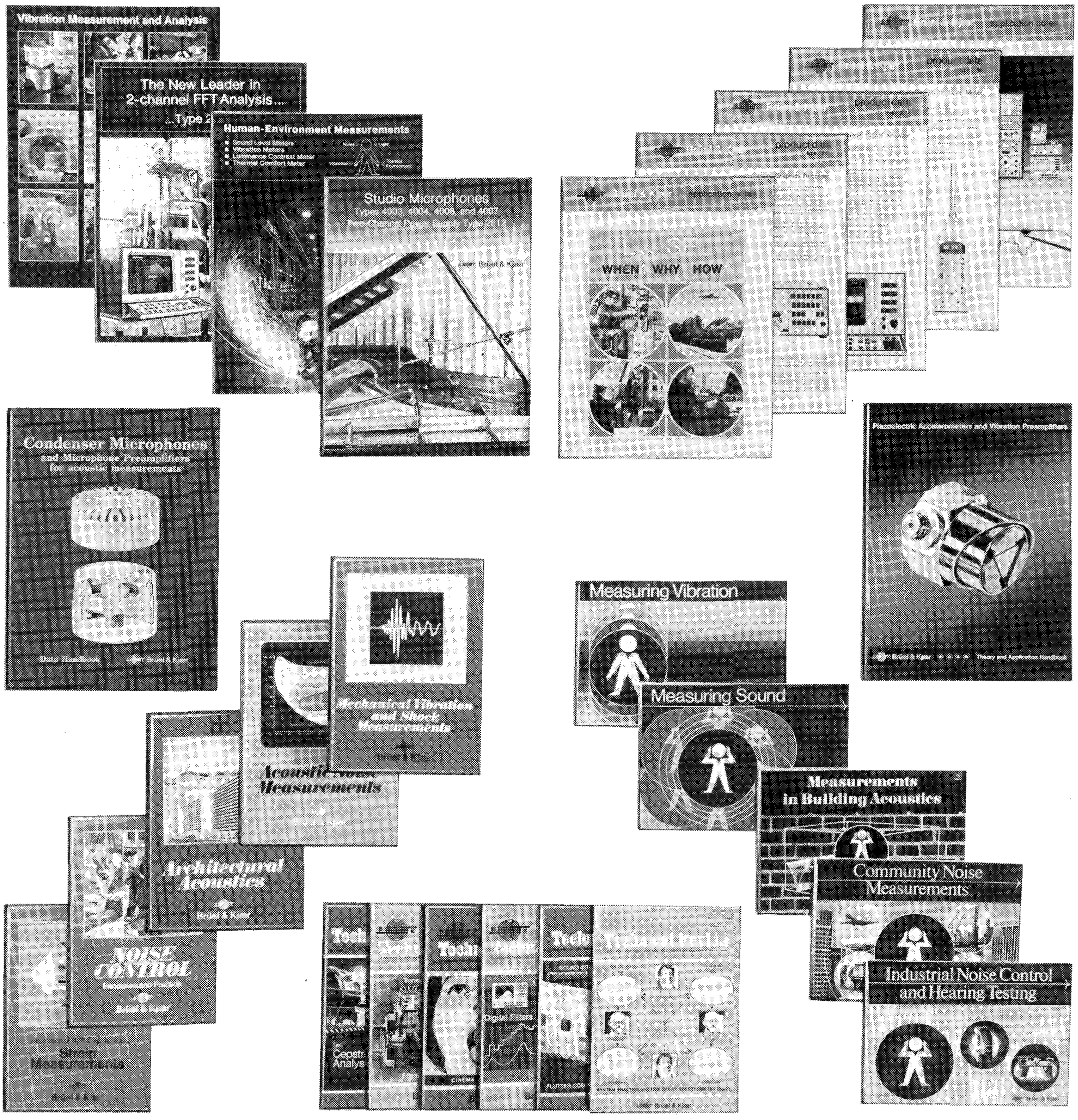

BV 0022-11

Brüel & Kjær

DK-2850 NÆRUM, DENMARK · Telephone: + 45 2 80 05 00 · Telex: 37316 bruka dk